293
116 pg $2.50

U. S. ARMY
TRANSPORTATION RESEARCH COMMAND
FORT EUSTIS, VIRGINIA

TRECOM TECHNICAL REPORT 64-12

FEASIBILITY INVESTIGATION OF HARMONIC DRIVE SPEED REDUCERS FOR HELICOPTER APPLICATIONS

Task 1D121401D14414
Contract DA 44-177-TC-716

May 1964

prepared by:

KAMAN AIRCRAFT CORPORATION
Bloomfield, Connecticut

DISCLAIMER NOTICE

When Government drawings, specifications, or other data are used for any purpose other than in connection with a definitely related Government procurement operation, the United States Government thereby incurs no responsibility nor any obligation whatsoever; and the fact that the Government may have formulated, furnished, or in any way supplied the said drawings, specifications, or other data is not to be regarded by implication or otherwise as in any manner licensing the holder or any other person or corporation, or conveying any rights or permission, to manufacture, use, or sell any patented invention that may in any way be related thereto.

DDC AVAILABILITY NOTICE

Qualified requesters may obtain copies of this report from

Defense Documentation Center
Cameron Station
Alexandria, Virginia
22314

This report has been released to the Office of Technical Services, U. S. Department of Commerce, Washington 25, D. C., for sale to the general public.

The findings and recommendations contained in this report are those of the contractor and do not necessarily reflect the views of the U. S. Army Mobility Command, the U. S. Army Materiel Command, or the Department of the Army.

HEADQUARTERS
U S ARMY TRANSPORTATION RESEARCH COMMAND
FORT EUSTIS, VIRGINIA 23604

This report represents a part of a continuing TRECOM research program for the investigation of new concepts of high-speed reducers for use as main transmissions in helicopters. The main efforts of this program are directed toward deriving a reduction unit or units, with a reduction ratio significantly higher (40:1 and above) than those of currently used transmissions, which would be more compatible with the high rotational speeds of aircraft turbine engines.

This Command concurs with the contractor's conclusions reported herein. Based on the results obtained from this specific study, the current design concept of the Harmonic Drive is not considered feasible for use as a helicopter main transmission. In the present state of the art, power losses associated with the hydrodynamic wave generator bearing prevent the achievement of the over-all efficiency that is present with conventional gearing or acceptable for helicopter main-drive train application.

This Command does not anticipate pursuit of the Harmonic Drive concept as such. However, a currently planned program of hydrodynamic bearing studies may produce results which would justify a reconsideration.

Wayne A. Hudgins
WAYNE A. HUDGINS
Project Engineer

J. Nelson Daniel
J. NELSON DANIEL
Group Leader
Aeronautical Systems & Equipment Group

APPROVED.

FOR THE COMMANDER:

Larry M. Hewin
LARRY M. HEWIN
Technical Director

Task 1D121401D14414
Contract DA 44-177-TC-716
TRECOM Technical Report 64-12
May 1964

FEASIBILITY INVESTIGATION

OF

HARMONIC DRIVE SPEED REDUCERS FOR

HELICOPTER APPLICATIONS

Kaman Report No. R-446

Prepared By

Kaman Aircraft Corporation
Bloomfield, Connecticut

For

U.S. ARMY TRANSPORTATION RESEARCH COMMAND
Fort Eustis, Virginia

PREFACE

This report covers the feasibility investigation of harmonic drive transmissions for helicopter applications (Contract DA-44-177-TC-716). This investigation was generated by the widespread application of gas turbine engines to helicopters which require speed reductions of over 50:1. Kaman Aircraft Corporation was the prime contractor with United Shoe Machinery Corporation, proprietors of the harmonic drive, as a contractually required subcontractor. The principals for this investigation were R. B. Bossler, Jr., Project Engineer, Kaman Aircraft Corporation; V. H. Meyer and P. C. Tappan, Project Engineers, United Shoe Machinery Corporation. The Contract Administrator at Kaman Aircraft Corporation was W. C. Kenyon, Jr. The Government representatives at U. S. Army Transportation Research Command, Fort Eustis, Virginia, were Lt. Colonel A. M. Steinkraus, Research Contracting Officer, and Mr. W. A. Hudgins, Project Engineer.

TABLE OF CONTENTS

LIST OF ILLUSTRATIONS

LIST OF TABLES

LIST OF SYMBOLS

A	Area in square inches
Ar	Area of flexspline bed in square inches
B	Length in direction of motion in inches
C_1	Constant of integration
D	Diameter in inches
Dpc	Pitch diameter of circular spline in inches
Dpf	Pitch diameter of flexspline in inches
d	Flexspline deflection in inches
E	Modulus of elasticity
e	Efficiency
F	Force in pounds
G	Modulus of shear
g	Acceleration of gravity (386 inches/second/second)
h	Oil film thickness in inches
h_{min}	Minimum oil film thickness in inches
Ip	Polar moment of inertia in inches^4
K	Proportionality constant
L	Length in inches
N	Angular velocity in r.p.m.
N_I	Input r.p.m.
Nd	Tooth difference
Nf	Number of teeth on fixed member

LIST OF SYMBOLS (Continued)

No	Number of teeth on output member
N_T	Transition number for laminar to turbulent flow, r.p.m.
P	Power in horsepower Pressure in p.s.i.
P_F	Probability of failure
R	Reliability Reduction Ratio
R_C	Rockwell Hardness Number, C Scale
Re	Reynold's number
R_I	Inside radius, undeflected flexspline
RMS	Root-mean-square deviations, surface roughness
r	Radius in inches
Sf	Flexure stress in p.s.i.
S_m	Mean stress in p.s.i.
Ss	Shear stress in p.s.i.
St	Tension stress in p.s.i.
T	Torque in pound-inches
Ti	Input torque in pound-inches
To	Output torque in pound-inches
t	Thickness in inches
U	Linear velocity in inches/second
V	Circumferential displacement in inches
v	Kinematic viscosity inches^2/second

LIST OF SYMBOLS (Continued)

Z	Viscosity in centipoises
α	Angle in degrees Dimensionless film thickness, h_{min}/B
γ	Angular displacement in radians
θ	Angle of twist per unit length in radians/inch
μ	Absolute viscosity in reyn (pounds seconds/inches^2)
ϕ	Angular position on wave generator in degrees

I. SUMMARY

The harmonic drive transmission achieves large speed reductions with only two major moving parts and promises great simplification as compared to conventional gearing in the speed reduction range required for turbine engines to helicopter rotors.

The research program reported herein has as its object the evaluation of the feasibility of using harmonic drive in Army helicopters in the following ways:

1. In auxiliary speed reducers, such as accessory drives, actuators, or rescue hoists;

2. In the main drive train between the engine and rotor.

Feasibility of the first class of application is believed amply demonstrated by the family of harmonic drive units which were developed and produced by United Shoe Machinery Corporation and their licensees for service use in servo actuators, radar antenna drives, and other similar applications. Experience gained in this research program further substantiates this belief.

Application to the helicopter main drive train is a much more critical requirement, and it was to this class of application that the principal effort in this program was addressed.

This report presents applicable helicopter and harmonic drive parameters, feasibility comparisons, data concerning the engineering and designing of a test unit, results of the test program, and recommendations for further research for improved efficiency.

A comparison of harmonic drive (H.D.) and conventional transmissions is presented over a range of from 250 horsepower to 4000 horsepower for the appropriate helicopter requirements. The harmonic drive shows advantages in reliability, maintainability, cost, noise, and weight. In general, these advantages increase with power. A serious disadvantage is relatively low efficiency; the efficiency can be improved, but this will require advances in the state of the art of high-speed/high-load bearing technology.

It is to be noted that conventional transmissions have been developed to a highly refined state, while H.D. is relatively new and undeveloped. H.D. may be expected to improve relatively rapidly with further research effort, therefore, while much more modest results are achievable with equivalent effort on conventional gearing. Potential efficiency, expected to result from further research in hydrodynamic bearing technology and flexspline design, is believed to approach that of conventional gearing. Substantial incentive for conducting further research exists.

II. CONCLUSIONS

As a result of preliminary studies, parametric analysis, and actual testing of a harmonic drive unit designed for 250 horsepower at 30,000 r.p.m. input speed with 85:1 reduction ratio, it is concluded that:

1. From the standpoints of compactness, quietness, vibration level, simplicity, reliability, and cost, harmonic drive appears to be not only feasible but superior to conventional planetary gearing.

2. In the present state of the art, power losses associated with the hydrodynamic wave generator bearing result in significantly lower efficiency than conventional gearing.

3. Acceptability for helicopter main drive train application would depend on trade-offs between Items 1 and 2 above for each specific application.

III. RECOMMENDATIONS

1. An improved mathematical model, more nearly representing the performance of the bearing under load and accounting for the individual and combined influence of the major parameters be developed.

2. More rigorous methods of stress analysis of the flexspline to provide better structural input data for design optimization be developed.

3. A harmonic drive transmission instrumented to measure stress distribution in the flexspline, film thickness distribution, and oil pressure distribution be tested further. These data are to be compared with predicted values from the mathematical model of Item 1 above for validation and refinement of the analytical methods.

4. With results of the above to use as a guide for theory and experiment, the benefits to be gained from modifications be explored.

IV. INTRODUCTION

The application of gas turbine engines to new designs of military helicopters and VTOL aircraft created the requirement for speed reduction between engine and rotor or propeller in excess of 50:1. Preliminary investigation indicated that harmonic drive transmissions might offer substantial advantages for high reduction systems in Army aviation.

USATRECOM initiated this program to determine the feasibility of the use of harmonic drive transmissions as main or auxiliary reducers in Army aircraft in response to an unsolicited proposal from Kaman Aircraft Corporation, an experienced helicopter manufacturer, to be supported by United Shoe Machinery Corporation, developer of the harmonic drive. This report presents the feasibility evaluation and describes the program on which it is based.

V. PROGRAM DISCUSSION

A parametric analysis established design conditions and helicopter design criteria for a comparative evaluation made of conventional and harmonic drive transmissions. This effort is reported in Section VI, A, Parametric Analysis - Turbine Helicopters, and Section VI, B, Design Criteria - Test Transmission.

This information was used to determine harmonic drive proportions and characteristics, revealing potential benefits and the need for experimental data. See Section VI, C, Parametric Analysis - Harmonic Drive.

A test transmission was designed and manufactured for the contractual conditions of 250 horsepower, 30,000 input r.p.m., 85/1 reduction ratio, and 1,000 hours of life. It was modified to facilitate efficiency testing. Engineering, design, and manufacture are reported in Section VII.

During the manufacturing period, a test bench was completed and the various systems were check-run.

Also during this period, supporting research was conducted on boundary layer lubrication to reduce starting torque and to permit operation of the hydrodynamic wave generator bearing in the incipient boundary layer zone where efficiency is highest. This investigation is reported in the Appendix. The test transmission starting torque was reduced by approximately one-third, as reported further in Section VIII, A, Starting Torque.

A test program was conducted with the 250-horsepower test transmission. Operation was exceedingly smooth and quiet. Design torque was easily transmitted. Lubrication and cooling were satisfactory. No mechanical or structural difficulties were experienced with the circular spline, flexspline, or shafting. Deterioration of the load-carrying surface of the wave generator hydrodynamic

bearing was overcome with a hardened nickel plate. Analysis of the test data established direction for size reduction to improve efficiency. The test program and evaluation are reported in Section VIII, B, Efficiency Investigation.

The test data were used to reproportion the family of harmonic drive transmissions, which were then compared to conventional transmissions to evaluate feasibility.

The evaluation of eight criteria is presented here as ratios of the harmonic drive (H.D.) values as compared to conventional (conv) reduction gearing transmission values. Where feasible, absolute values are also included. The direction of changes resulting from research to improve efficiency will reduce harmonic drive diameter, length, weight, and effective weight below the values presented at this time. Reliability, noise, and cost ratio should remain essentially unchanged.

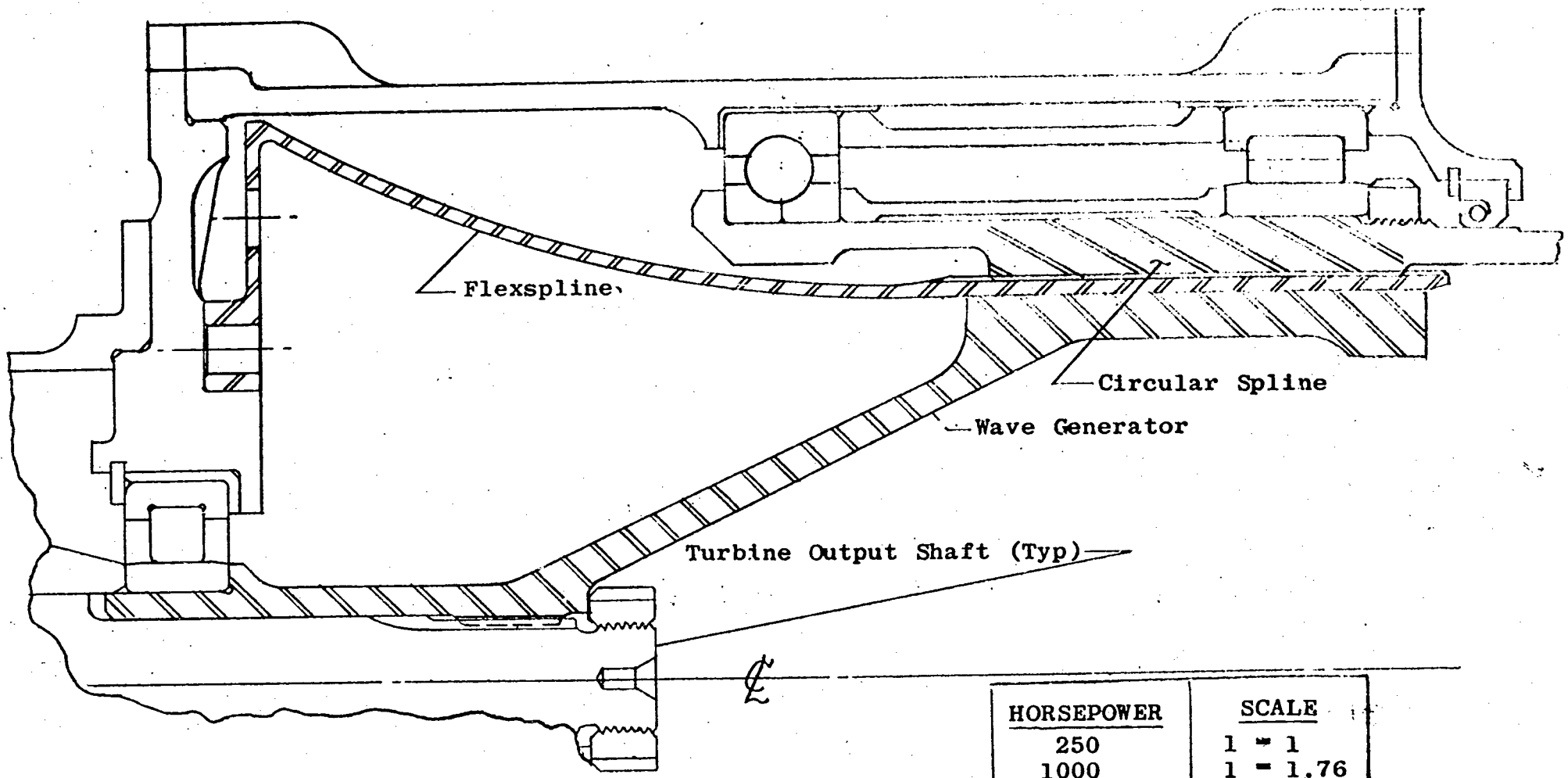

HORSEPOWER	SCALE
250	1 = 1
1000	1 = 1.76
2000	1 = 2.38
3000	1 = 2.87
4000	1 = 3.23

Figure 1. Harmonic Drive Turbine/Helicopter Speed Reduction Design Per Test Unit Design Critique

1. Reliability

$$\frac{\text{H.D. Probability of Failure}}{\text{Conv. Probability of Failure}} = \frac{3.7}{10}$$

This ratio is approximately constant from 250 horsepower to 4,000 horsepower.

2. Noise Ratio

Noise level measurements were not taken. Noise could not be detected with a conventional stethoscope during testing. Background noise was present during the test. Compared to conventional transmission, the harmonic drive is extremely quiet and vibration free.

3. Cost Ratio

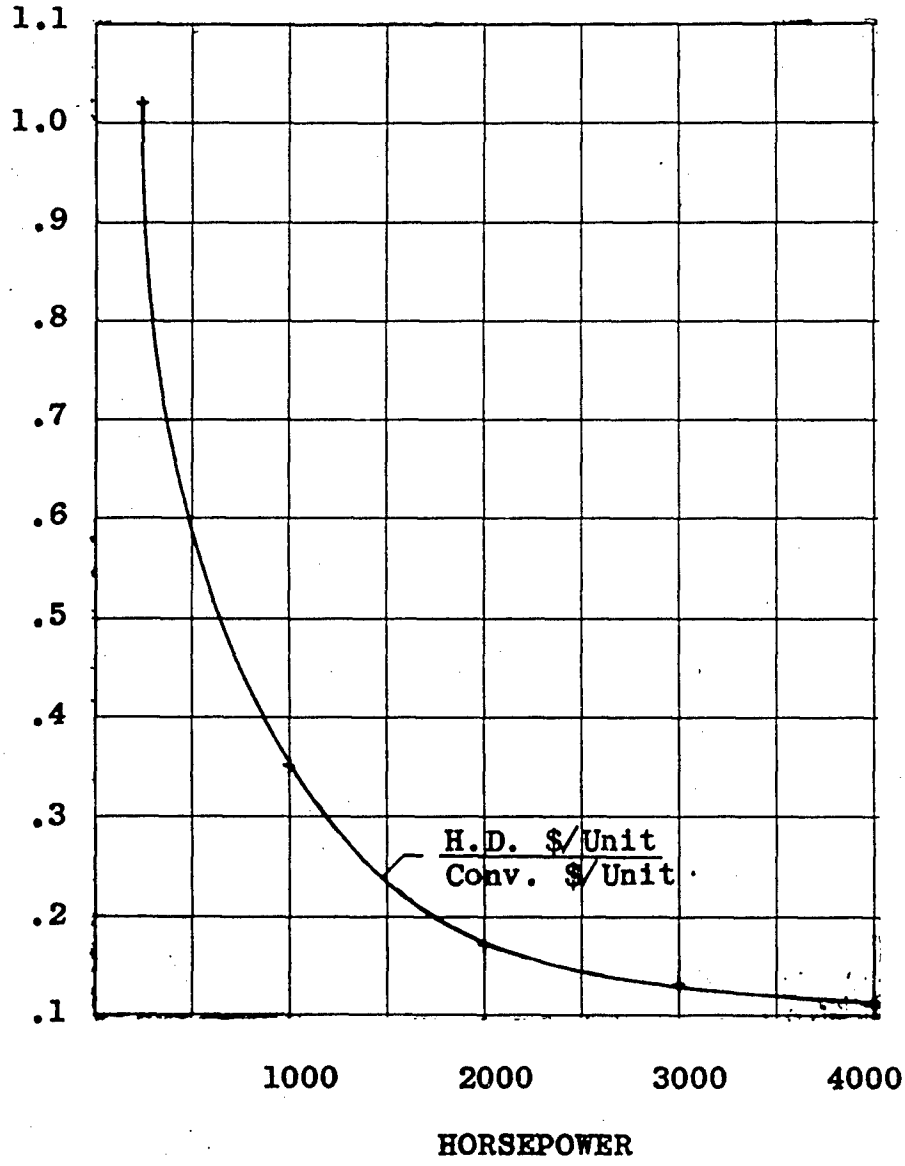

Figure 2. Cost Ratio Versus Horsepower

4. Diameter

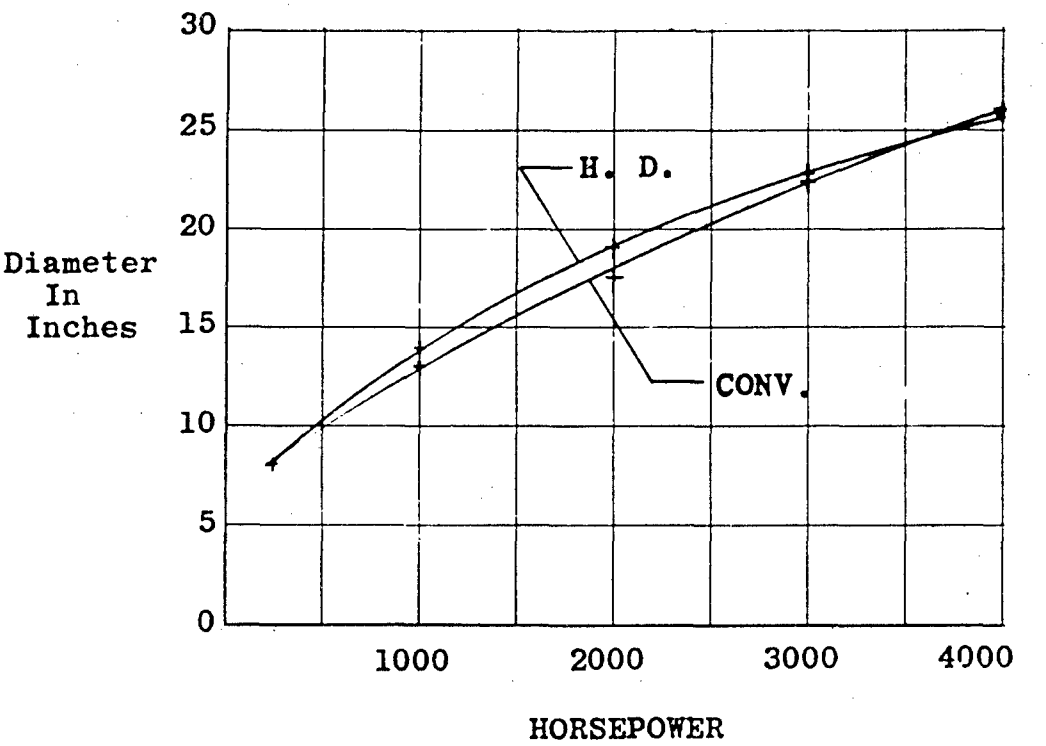

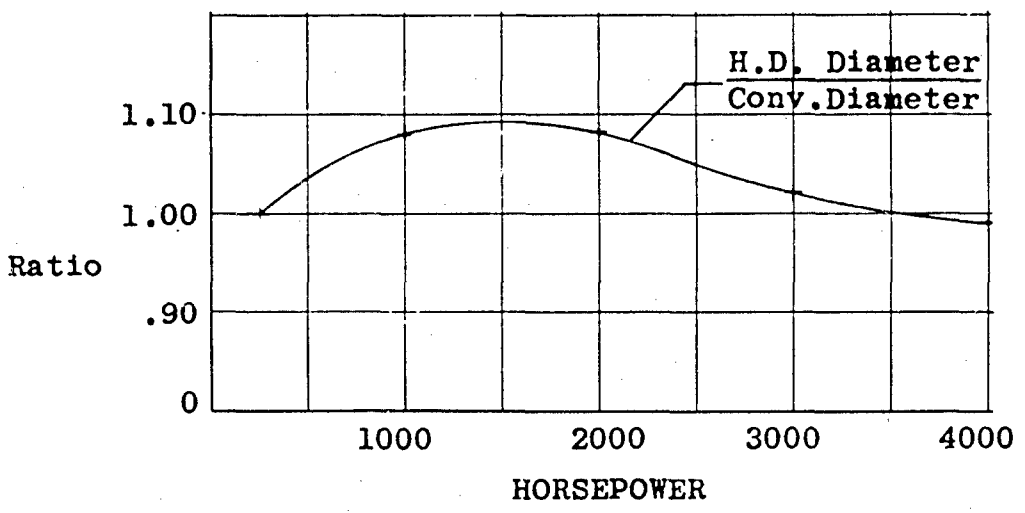

Figure 3. Diameter Versus Horsepower

5. Length

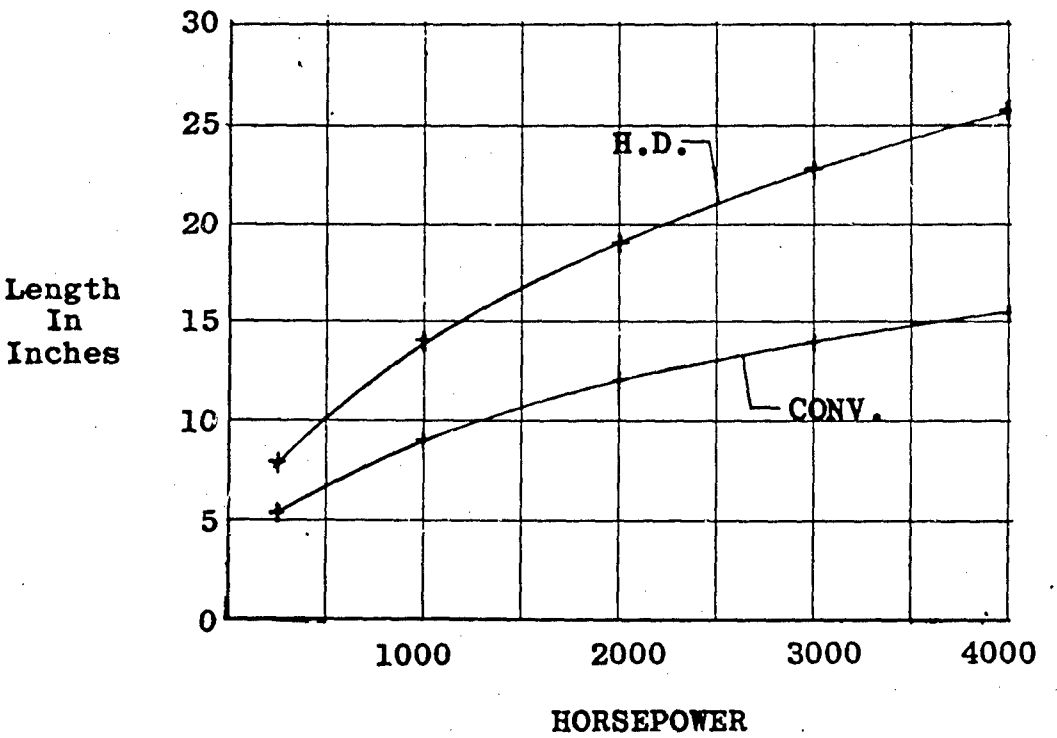

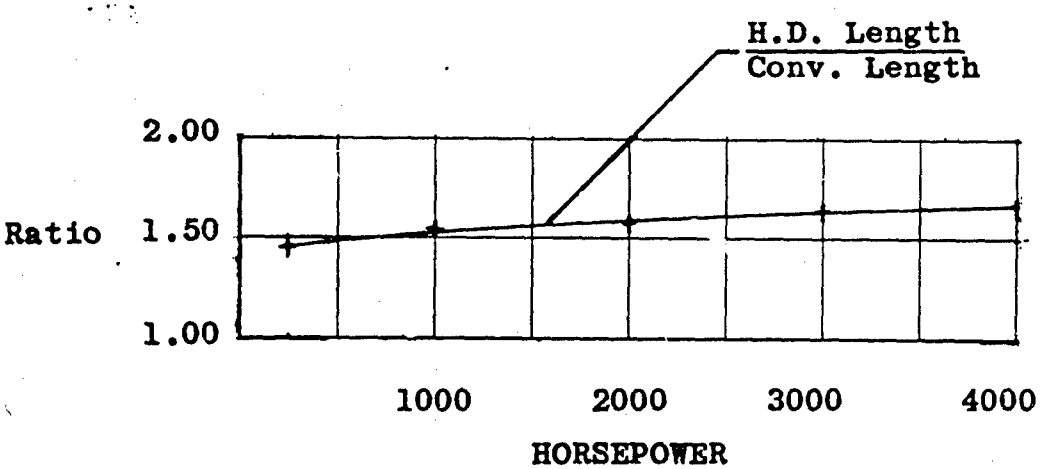

Figure 4. Length Versus Horsepower

6. Weight

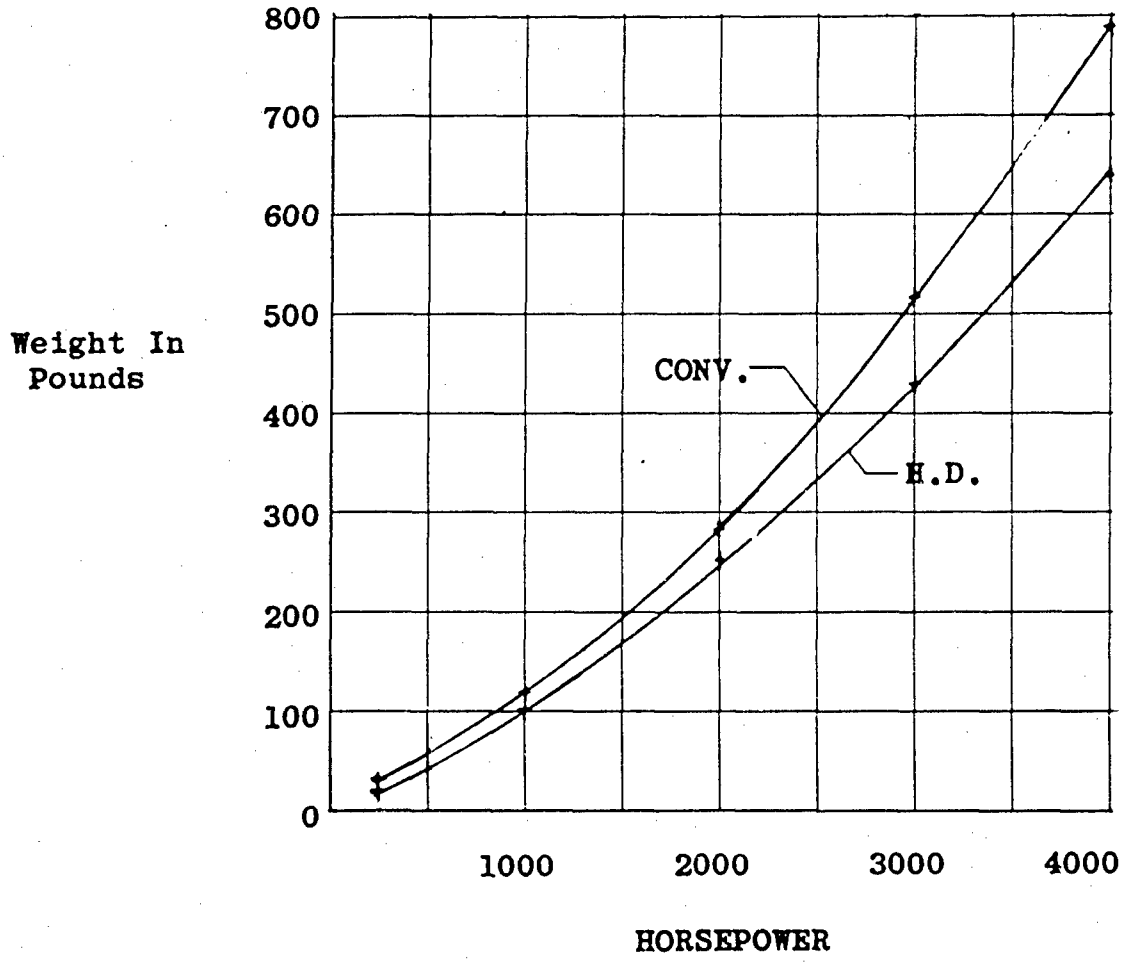

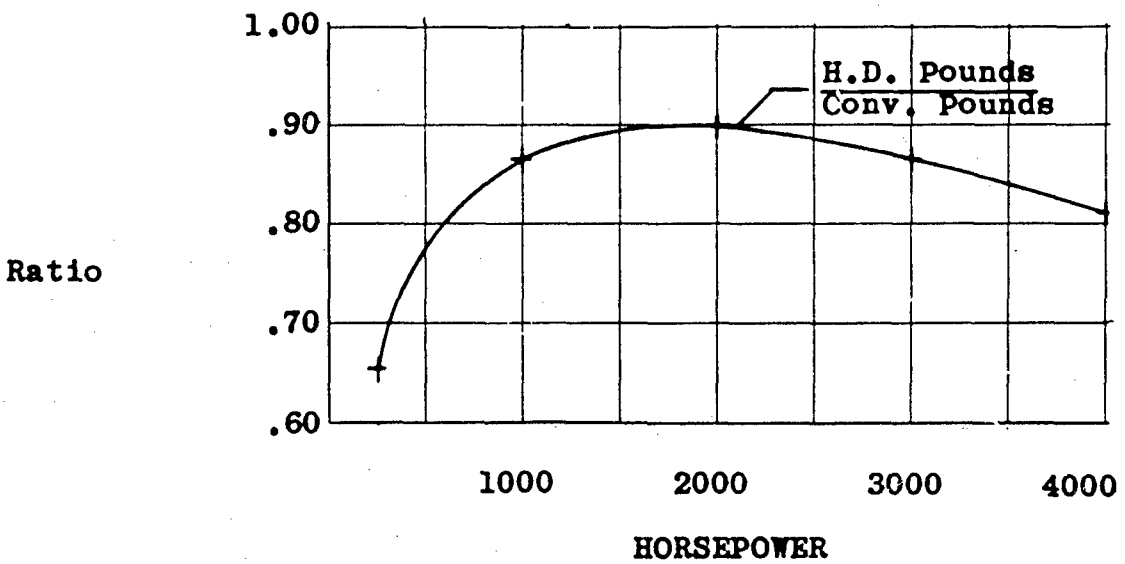

Figure 5. Weight Versus Horsepower

7. **Efficiency**

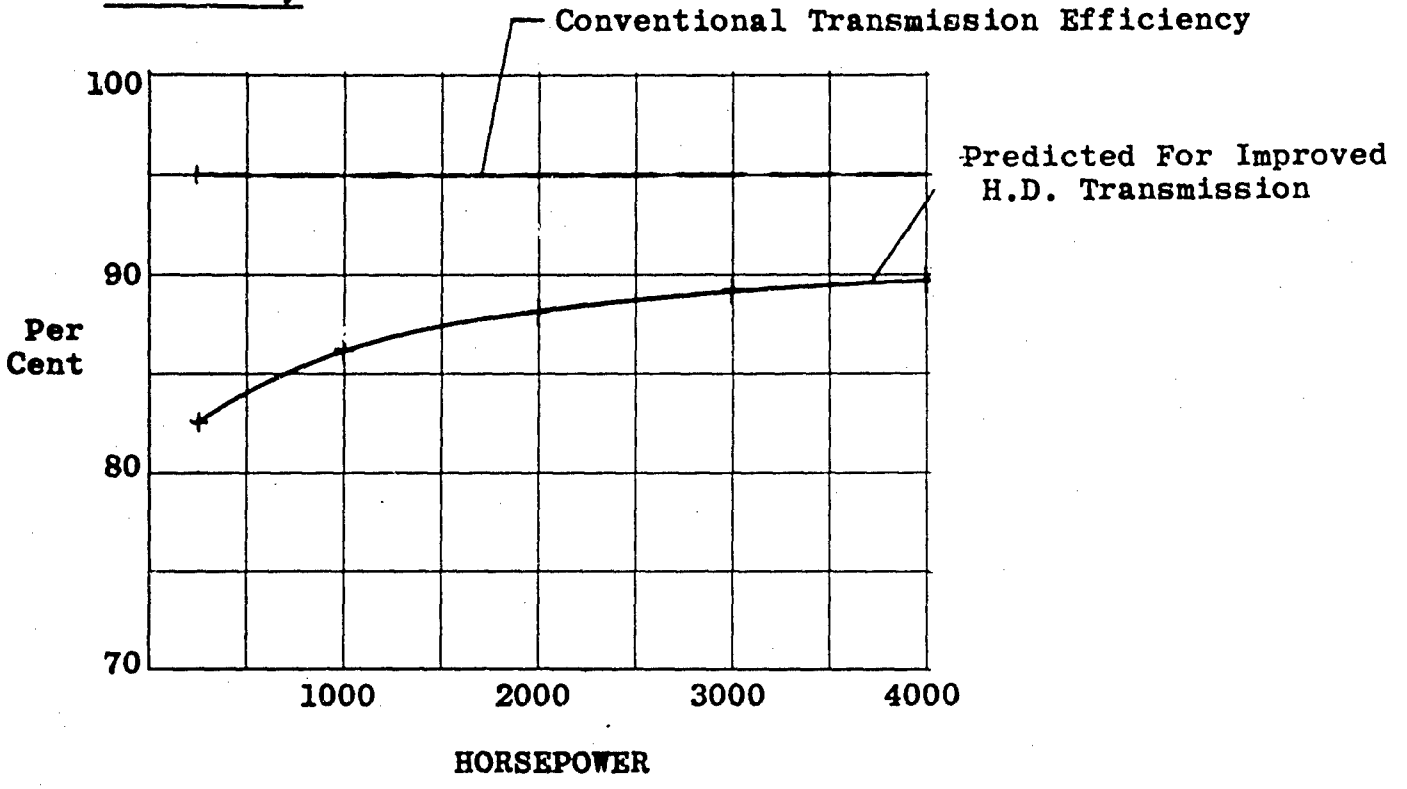

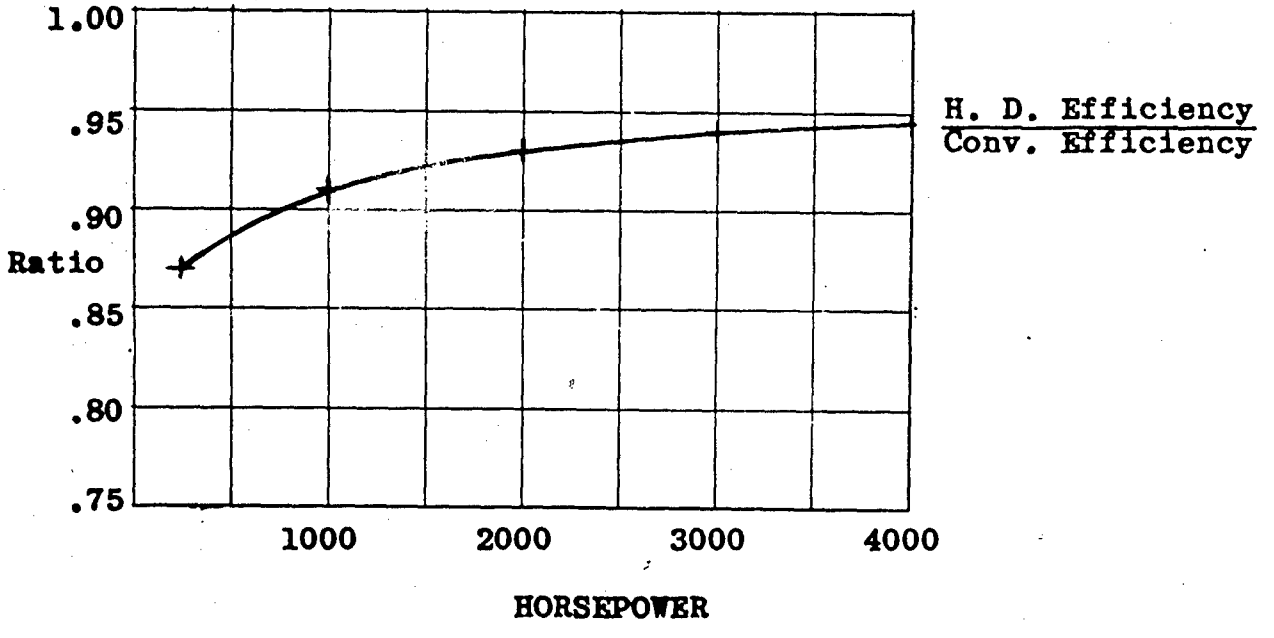

Figure 6. Efficiency Versus Horsepower

8. Effective reduction gearing weight = actual weight of main reduction gearing elements plus losses converted to weight at 8 pounds per horsepower.

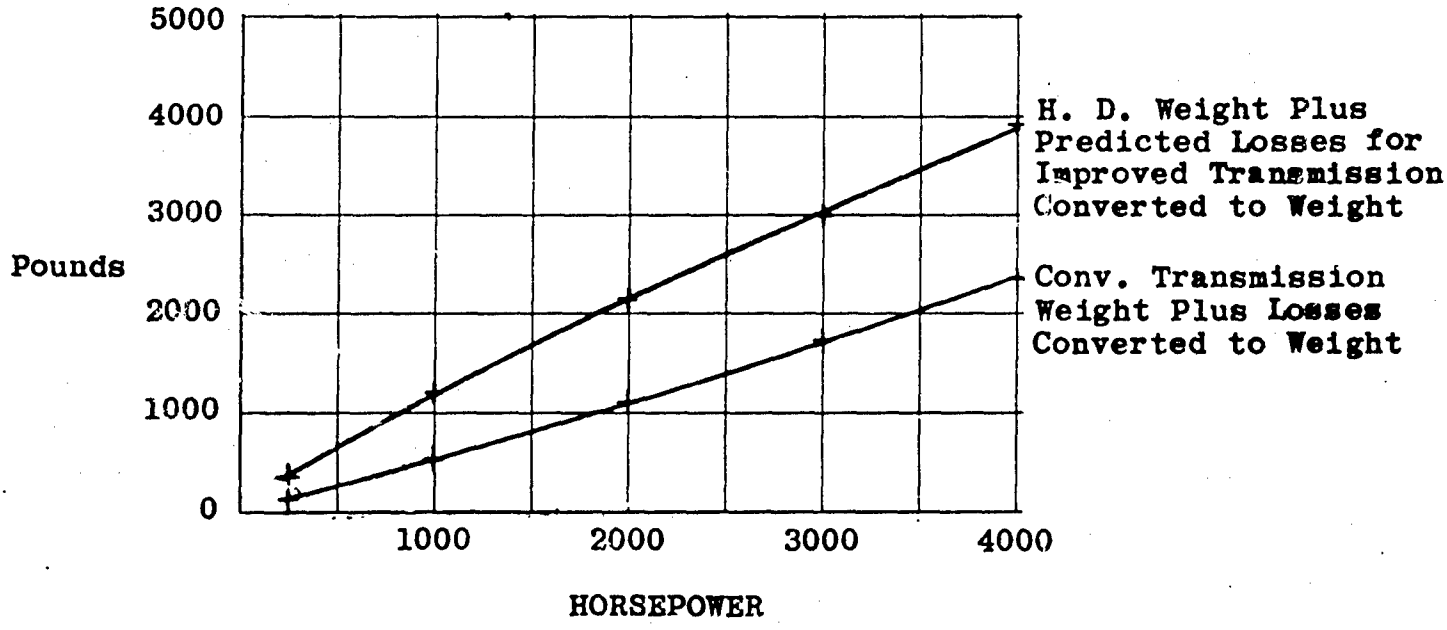

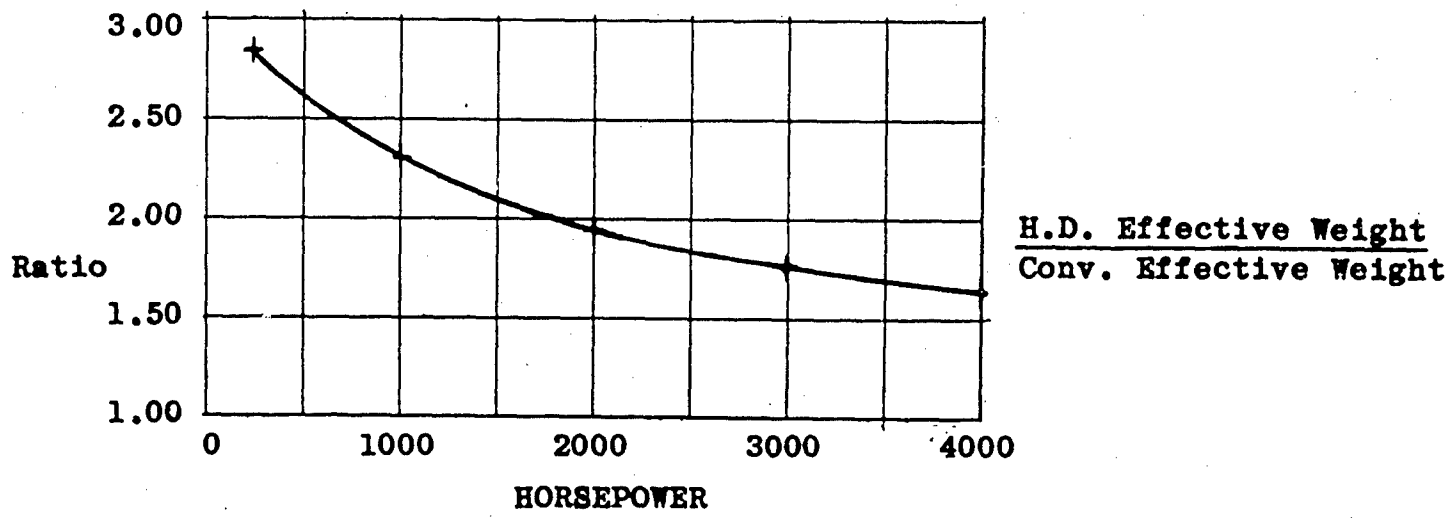

Figure 7. Effective Weight Versus Horsepower

VI. ANALYSIS OF PROBLEM

A. PARAMETRIC ANALYSIS - TURBINE HELICOPTERS

The purpose of this parametric analysis is to establish reasonable requirements to be used to evaluate the harmonic drive transmission for helicopter applications. This analysis is fixed in origin at 250 horsepower, 30,000 r.p.m., and 85/1 reduction ratio. The suggested limit was 2,500 horsepower. The limit selected is 4,000 horsepower.

This analysis reveals an interesting situation. In general, both turbines and rotors are controlled by the same parameters. To increase power, radius must increase. Since tip speed is limited, r.p.m. must decrease. An alternate to increasing radius is to increase the number of blades in helicopter rotors and the number of stages in turbines. This leads to variations which are the result of individual decisions as to the most advantageous compromise. These tend to be historical trends. For example, if a company has a working two-bladed rotor, they scale it up for an increase in power. The resultant low solidity requires a high tip speed to compensate for it. We then have a variation at the power level where other designs use three or four blades.

Figure 8, rotor r.p.m. versus horsepower, shows the anticipated future rotor r.p.m. envelope. The philosophy applied to establish a most probable curve is as follows: at lower horsepower, structural problems are not as severe as are efficiency requirements. Therefore, a most probable curve would tend toward the low disc load, low solidity, and low tip speed boundary. At high horsepower, structural problems become intense and the rotor radius becomes limited. The most probable curve would tend toward the high disc load, high solidity, and high tip speed boundary. Helicopters allow greater freedom of design than turbines and exhibit greater variations.

Figure 9, turbine r.p.m. versus horsepower, shows how much more closely turbine r.p.m. correlates with increasing power, at least in the higher ranges. If r.p.m. versus power were consistent, the curve would be a hyperbola asymptotic to the zero axes. It should be noted in establishing a most probable curve that historically a given engine grows in power without change in r.p.m., as metallurgical improvements permit higher inlet temperatures.

Figure 10, input-output r.p.m. versus horsepower, shows the superimposed most probable curves of turbine and rotor r.p.m. versus horsepower. For the purposes of this general analysis, the reduction ratio is also thus established. This reduction ratio can be treated as reasonably constant at 85/1 through the range from 250 horsepower to 4,000 horsepower. This constant ratio greatly simplifies the study in that parts can be scaled up or down without changing internal relationships.

In order to provide a rational evaluation of the harmonic drive, Figure 10 data were used to design an alternate reduction system, in-line reduction units with no provisions for a free-wheeling unit, change of direction, and auxiliary drives. This study evaluates the speed reduction function of conventional helicopter transmission requirements.

A four-stage planetary was chosen. This was simplified by using a constant reduction ratio/stage. For this study, the fourth, or output, stage has six planets proportioned by output torque. The third stage, carrying one-third of the torque, has two such planets. The second stage, carrying one-ninth of the torque, has six planets with one-ninth the face width. The first, or input stage has two planets of the same proportions as the second stage planets. It is realized that the first (input) stage would not be proportioned by torque. It is felt that the parameters so derived permit broad evaluation for comparative purposes without requiring the detailed treatment of an actual unit. The 250-horsepower unit is shown on Figure 11. Units were similarly proportioned for 1,000, 2,000, 3,000, and 4,000 horsepower. Figure 12 presents conventional reduction gearing parameters which were derived by this study versus horsepower.

A general survey of the field established 5-percent losses as a reasonable value. This 95-percent efficiency is treated as constant.

Two parameters, actual weight and efficiency, are also evaluated simultaneously in terms of total effective weight, where

Total effective weight = Actual weight + Horsepower loss x 8 lb/hp.

For the planetary system, as evaluated, this becomes

Total effective weight $\simeq$ horsepower (0.2 lb/hp + 0.05 x 8 lb/hp),

or total effective weight $\simeq$ 0.6 lb/hp.

Cost ratio analyses exclude engineering and tooling and assume the same rate of cost decrease with quantity.

Reliability of the harmonic drive is assessed on a comparative rather than on an absolute basis. The multistage planetary design is assigned an over-all reliability factor of .900. Its 63 elements are then grouped into nine categories and assigned factors compatible with the over-all R = .900.

Similar factors are then applied to the six categories of the 22 elements of the harmonic drive; this gives, by application of the product rule, an over-all reliability of R = .963.

In terms of probability of failure (P_F = 1 -R), the harmonic drive shows 3.7 percent compared to 10 percent for the conventional reduction system - a gain of almost 3 to 1. Because the requirement for corrective maintenance varies directly with the probability of failure, it is obvious that a proportionate reduction in maintenance is achieved by the harmonic drive.

These considerations of effective weight, cost ratio, and reliability ratio must be integrated into an over-all evaluation. For instance, an increase in effective weight may be acceptable in view of the large gain in reliability and maintainability.

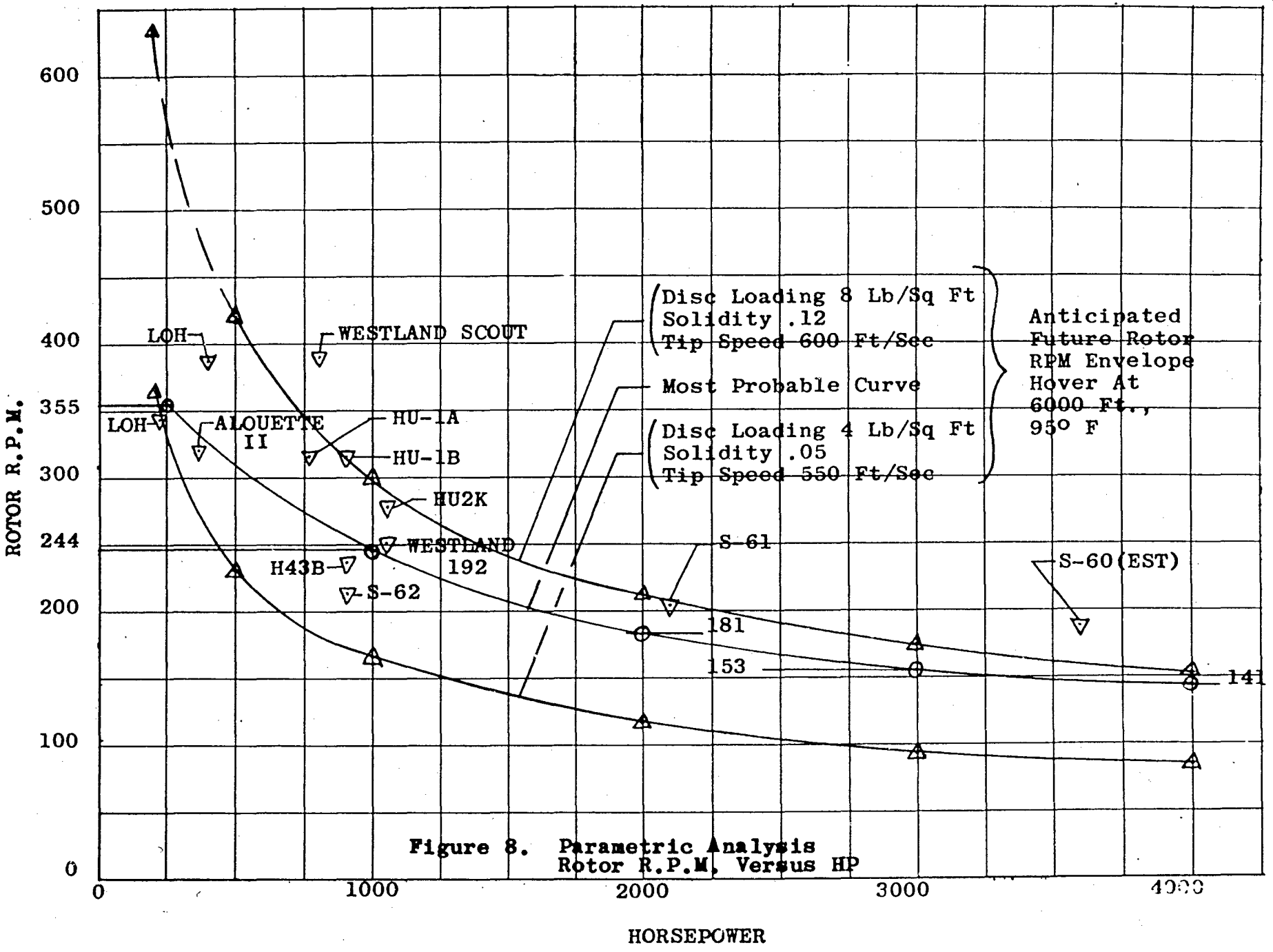

Figure 8. Parametric Analysis Rotor R.P.M. Versus HP

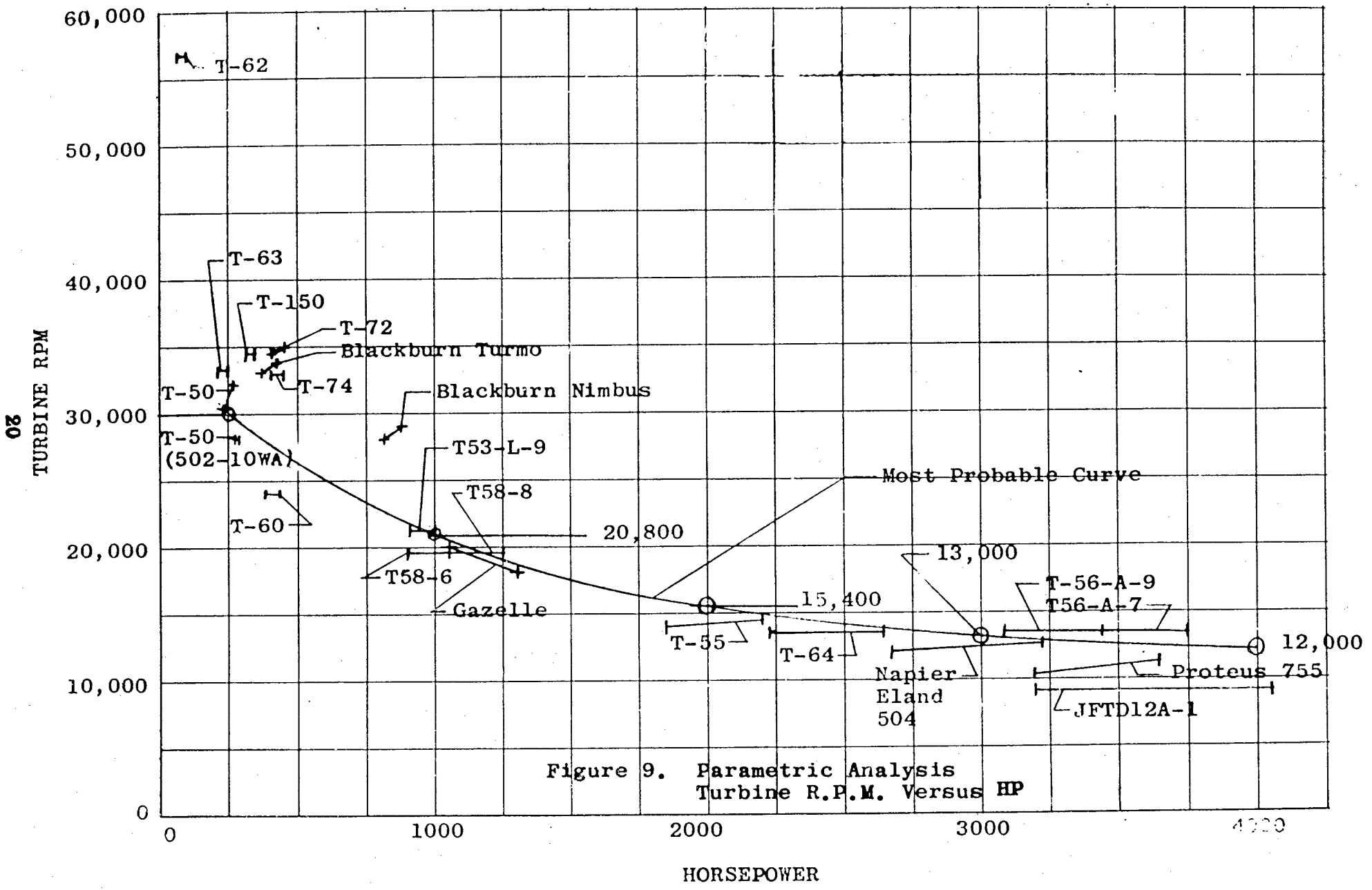

Figure 9. Parametric Analysis
Turbine R.P.M. Versus HP

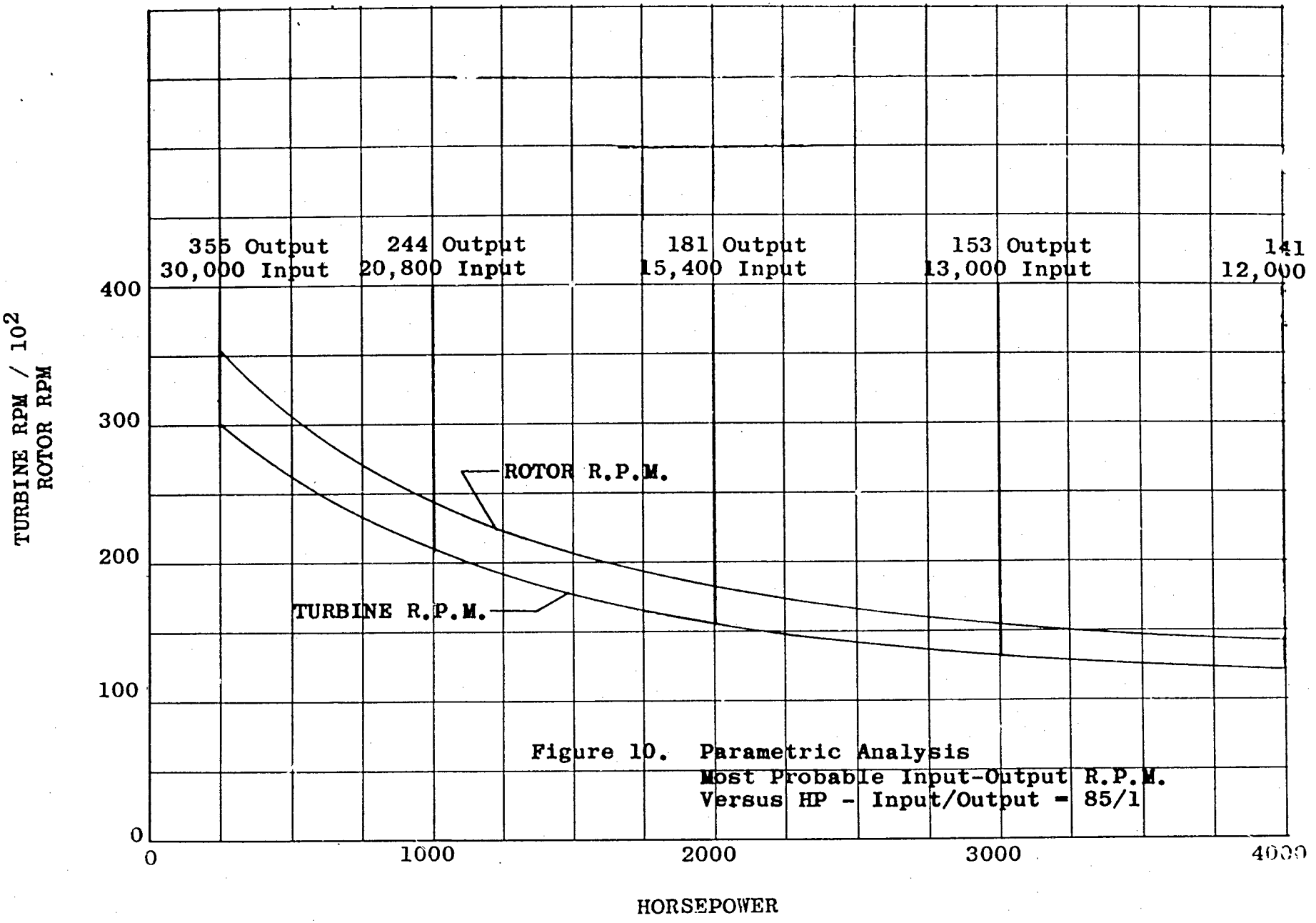

Figure 10. Parametric Analysis
Most Probable Input-Output R.P.M.
Versus HP - Input/Output = 85/1

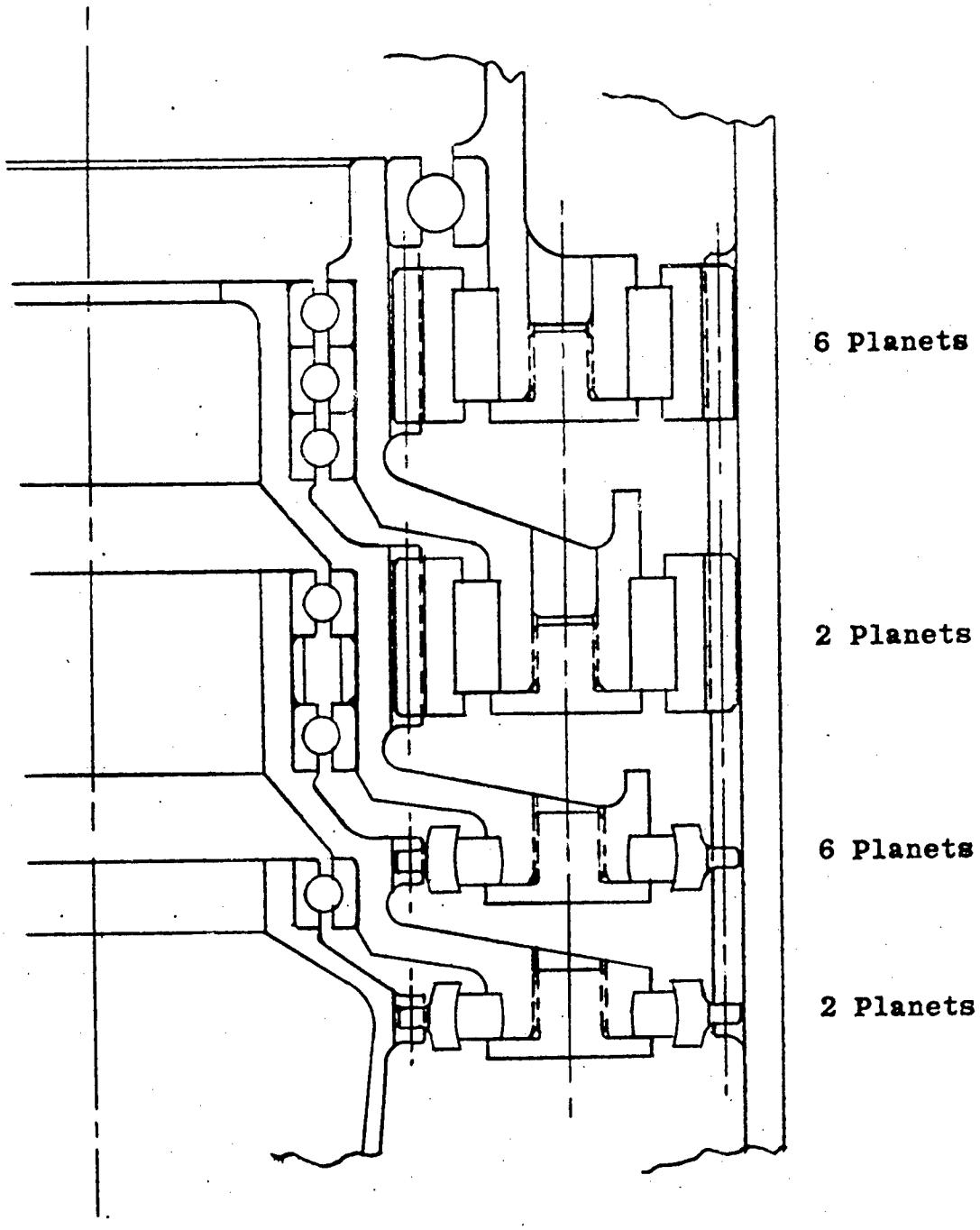

Figure 11. Parametric Analysis - Conventional Reduction Gearing - 250 Horsepower

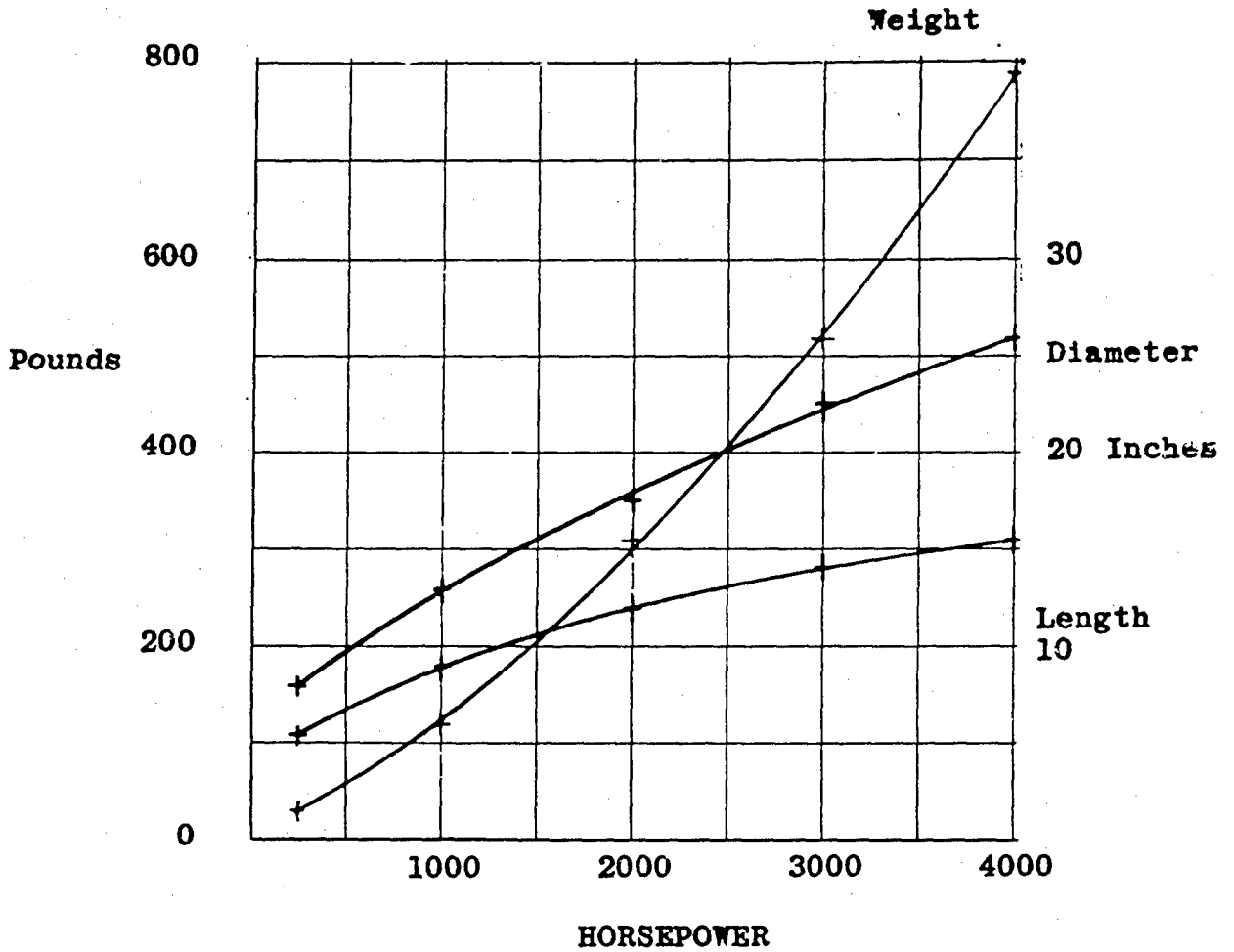

HORSEPOWER	WEIGHT	DIAMETER	LENGTH
250	29	8.0	5.5
1000	119	13.0	9.0
2000	310	17.5	12.0
3000	518	22.5	14.0
4000	790	26.0	15.5

Figure 12. Parametric Analysis-Conventional Reduction Gearing Parameters Versus Horsepower

B. HELICOPTER DESIGN CRITERIA FOR HARMONIC DRIVE TEST TRANSMISSION

The following have been established as general requirements for helicopter design and for the harmonic drive test transmission:

(1) Design torque = maximum steady-state operation condition. Corresponds to 250 horsepower at 30,000 r.p.m. input.

(2) Limit torque = 200 percent maximum design torque.

(3) Ultimate torque = 150 percent x (2) = 300 percent x (1).

(4) Assume no flywheel resonance problem.

(5) Cyclic torque components will be present at frequencies corresponding to output frequency and integral multiples thereof. Amplitude of components will probably decrease sharply with frequency, orders above the sixth being usually negligible. It should be assumed that the peak-to-peak wave form will be contained within the envelope of $\pm$10 percent of design torque.

(6) Operating torque is from 50 percent to 100 percent design torque, with only very short term transients above 100 percent design torque. (Assume impacts are not a factor because of limit torque requirement.) Design of expendable parts (parts of relatively low value and with predictable failure patterns replaced at overhaul) may make use of the following prorating schedule for fatigue design:

Operating Condition	Percent Of Design Torque	Percent Of Total Operating Time
Vmax (or max rate of climb)	100	30
Hover	61.5	45
Cruise	55.5	25

This schedule is usually used only for rolling contact bearings. The designed 10-percent failure life for bearings should be 1,200 hours minimum. All gearing, shafts, splines, or other mechanical elements which contribute to a major portion of the foreseeable cost of a final production design shall be designed for infinite fatigue life at design torque.

(7) Temperature: -65°F to 180°F. The ship must fly without warmup. It is felt that the design is not to be compromised to meet this environment, although it should be recognized as an ultimate objective. Such limits as are required will be noted.

(8) Total vibration level shall be ±0.3 G and will occur at integral harmonics of output frequency.

(9) Transient acceleration level shall be -0.5 G to +3 G along the axis of harmonic drive.

(10) Starting inertia and acceleration to speed shall be figured from three 17-foot blades at 60 pounds each with the weight concentrated at an 8-1/2-foot radius.

(11) The transmission mount shall be undefined at this time. A general configuration will become apparent as design work progresses.

(12) An accessory drive gear will be present in any practical helicopter transmission and will be located between transmission output and rotor. The details of this gear location and description will not be determined.

(13) Rotor and fuselage loads, including crash loads, will be isolated from the transmission except as noted.

C. PARAMETRIC ANALYSIS - HARMONIC DRIVE

Introduction

The operating principles and performance capabilities of harmonic drive are described in detail in a number of publications (References 2 and 6). Only a brief summary is given here as background. A single harmonic drive stage generally consists of three basic elements:

(1) The Wave Generator shown in Figure 13(a) commonly has and "elliptoidal" (or ellipse-like) shape and is surrounded by a bearing for the transfer of this shape.

(2) The Flexspline, a flexible (normally metallic) part with external teeth, shown in Figure 13(b), is deflected into elliptoidal shape by the wave generator.

(3) The Circular Spline, shown in Figure 13(c), is rigid and circular with internal teeth and mates with the flexspline, as shown in Figure 13(d), at two diametrically-opposed regions located at the major axis of the elliptoid. At the minor axis the teeth of the flexspline and the circular spline are disengaged and clearing.

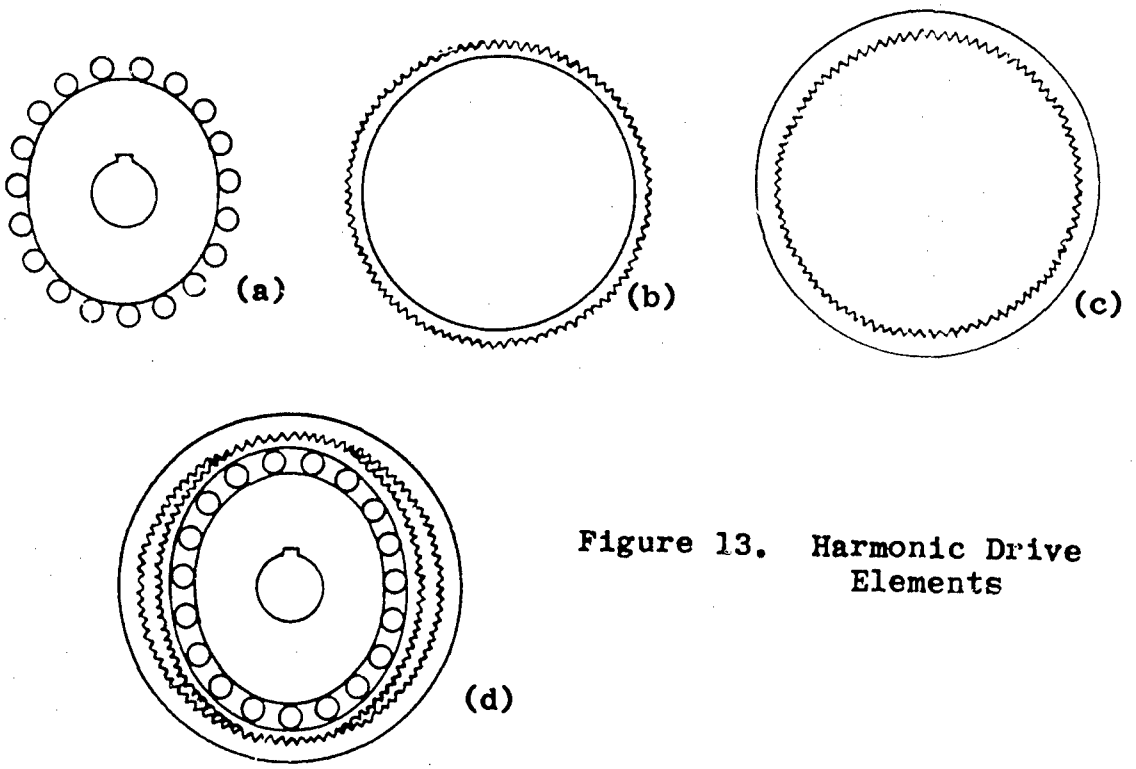

Figure 13. Harmonic Drive Elements

Assuming the rigid circular spline to be held stationary, rotation of the wave generator causes a progressive rotation of the elliptoidal shape in the flexspline, resulting in a continuous and progressive interengagement between flexspline and circular spline teeth. There are fewer teeth on the flexspline than on the circular spline, and a slow mechanically reduced relative motion between these two elements is thus generated. By any of a number of means, rotational motion of the flexspline is smoothed (averaged) and coupled out to a rotating shaft.

Discussion

This analysis presents a harmonic drive concept which utilizes a hydrodynamic wave generator bearing. Parameters are established and evaluated for a series of reducers ranging from 250 horsepower at 30,000 r.p.m. input to 4,000 horsepower at 12,000 r.p.m. input, all with a reduction ratio of 85/1.

A hydrodynamic wave generator bearing was chosen because the diameter and length of the flexspline required to carry the output torque appear to preclude the use of ball or roller wave generator bearings. The most common type of wave generator bearing is a ball bearing between the wave generator and flexspline, as shown on page 26. This type would reach a DN value of about 3,000,000 at 30,000 r.p.m. with .375-inch-diameter balls. This number, at the present state of ball bearing technology, is prohibitive, especially when the bearing radial load is considered. A second approach uses eccentrically mounted ball bearings with large wheel-like outer races to extend out to the flexspline. This has the advantages of a lower DN value (the major axis load can be reacted by centrifugal force), and the rigidity of the wheel provides better load distribution among the balls than does the flexspline acting as the outer race. The design is quite complex, however, and provides support at the major axis only. This latter characteristic disqualifies the design for high torque applications. This study establishes the feasibility of the hydrodynamic wave generator bearing approach.

The thin-walled flexspline of the harmonic drive may deflect slightly from its optimum elliptoidal shape to produce relatively thick hydrodynamic films in regions of small radial load, and thin films in regions of large load. It is believed, therefore, that the wave generator's operating and loss characteristics will be more analagous to those of a Kingsbury type thrust bearing with its tilting pads than to those of a shaft in a journal bearing.

This assumption eliminates a number of successive approximation steps necessary to developing wave generator contours having minimum loss characteristics. The Kingsbury bearing formulas assume that the film thicknesses will automatically adjust themselves to optimum contours.

This analysis uses formulas and information obtained from Shaw and Macks "Analysis and Lubrication of Bearings" and from Wilcock and Booser "Bearing Design and Application", References 4 and 5.

Addendum

This harmonic drive parametric analysis was and is useful in defining trends and problem identification. The information contained here is largely superseded by later developments. For instance, diameters may be reduced below the values presented; the limit of film thickness reduction is unknown, but believed to be less than the .001 inch assumed here; and the practical limit of viscosity reduction is set by JP-4 to range from 0.9 to 0.6×10^{-7} reyns rather than the 2.75×10^{-7} reyns assumed in Curve F.

These are changes of degree, not of kind. The essential conclusion reached, Curves H and I, is that Horsepower Loss = (Constant) (Output Torque)$^{5/6}$ (Input Speed). This is believed to be a valid definition when used for the purpose of defining the present state of the art.

1. Parameters and Results

The results of the harmonic drive parametric analysis are shown in Figure 14. The substantiating data are presented in Table I. The results are evaluated immediately after the parameter description.

The abscissa is established by definition as 0 to 4,000 horsepower. The limits of this investigation are 250 to 4,000 horsepower.

Design Conditions (Curves A, B, and C)

Input Speed, Curve A, was taken from Figure 10 data. Output Torque, Curve B, was calculated using Figure 10 data. Diameter, Curve C, was then calculated.

$$D_{PC} = \frac{T_o^{1/3}}{7}$$ Harmonic drive design standards

where D_{PC} = Circular spline pitch diameter

T_o = Output torque

The test transmission used D_{PC} = 5.375 inches and was slightly larger than calculated by this method. The resultant flexspline inside diameter is 5.0625 inches. In this analysis, 5.07 inches are used as D for both circular spline pitch diameter and flexspline inside diameter, ignoring the small error. Note in Figure 14 that the diameter increases from about 5 inches at 250 horsepower to 17.50 inches at 4,000 horsepower.

Generator Length (Note Plotted)

The working length of the wave generator is equal to its diameter in this study. In order to avoid abrupt pressure variation under the ends of the spline teeth, the test transmission wave generator is six inches long, extending one-half inch beyond the circular spline teeth at each end.

Minimum Film Thickness (Curves D and E)

This is the thickness of the oil film between the wave generator lobe (major axis diameter) and flexspline, and occurs under the engaged driving teeth.

This analysis uses film thickness increase with the square root of the diameter; thus,

$$h_{min} = 6.7 \times 10^{-4} D^{1/2} = 2.53 \times 10^{-4} T_o^{1/6}$$

Viscosity (Curves F and G)

In these formulas, the viscosity μ of the lubricant is given in reyns. The viscosity is calculated from a series of formulas and graphs in Reference 5. Reducing the viscosity reduces the film thickness and increases the efficiency. For instance, the reduction of h_{min} from .0015 to .001 inch could be accomplished by reducing μ from 5.75×10^{-7} reyns to 2.75×10^{-7} reyns. Oil of $\mu = 5.75 \times 10^{-7}$ reyns would be a very light gas turbine bearing oil. Oil of $\mu = 2.75 \times 10^{-7}$ reyns is about equal to kerosene. From the above it can be seen that the oil viscosity appears to be reduced to its practical limit.

Efficiency (Curves H and I)

The test transmission is working in a critical range. Anything smaller, with a corresponding increase in input speed, would be very inefficient. Larger units become more efficient.

These curves indicate that a major part of our effort should be devoted to improvement in hydrodynamic bearing performance.

Turbulence

This study has assumed laminar flow in the oil film. If the flow is turbulent, the losses will be much greater than the curves indicate. The available analyses, References 4 and 5, are based on empirical data whose applicability to the present case may be questioned. The effect of the flexible nature of the bearing may be significant. The circumferential pressure distribution is qualitatively different from journal bearings. Further, the references cited note the lack of suitable theory, even for conventional journal and thrust bearings, and the need for experimental research. Under these conditions, predictions will be dubious until adequate theory or specific test data are available.

Evaluation of Results

Improvement in the efficiency of the hydrodynamic bearing is required in order to realize the many harmonic drive advantages in vibratory behavior, size, weight, reliability, maintainability, and cost; although, it should be noted that present predictions of efficiency are based on only approximate methods of analysis. Improvement can be expected from identification of significant bearing parameters and a better understanding of their influence. The parameters which are believed to be important are lubricant viscosity, bearing velocity, and bearing load-carrying capacity. The test program is expected to determine their influence. It may identify other parameters and determine the adequacy of the conventional methods of analysis now applied to the known parameters.

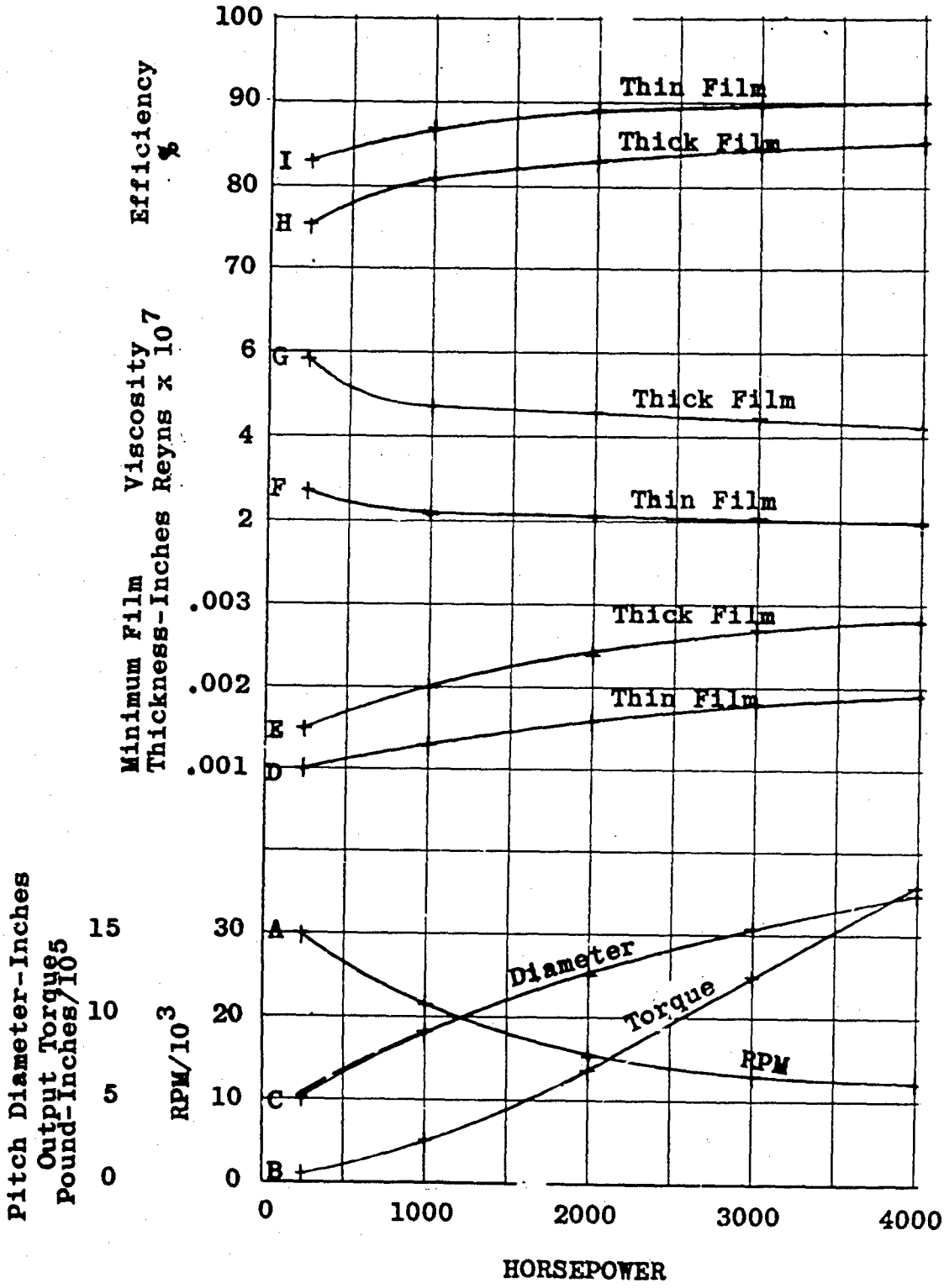

Figure 14. Harmonic Drive Parameters Versus Horsepower

TABLE I

HARMONIC DRIVE PARAMETRIC DATA

HP	250	1,000	2,000	3,000	4,000
R.P.M.	30,000	20,800	15,400	13,000	12,000
T_o	44,600	257,000	695,000	1,235,000	1,785,000
D	5.07	9.1	12.65	15.35	17.35
h_{min} (thick)	.0015	.002	.0024	.0027	.0028
h_{min} (thin)	.001	.0013	.0016	.0018	.0019
$T_o^{5/6}$	7,500	32,000	74,000	119,000	160,000
HP Loss (thick)	81	239	410	556	691
Input	331	1,239	2,410	3,556	4,691
Eff.	75.5	80.7	83	84.5	85.4
HP Loss (thin)	51.7	153	252	356	442
Input	301.7	1,153	2,252	3,356	4,442
Eff.	83	86.7	89	89.5	90
$T_o^{1/3}$	35.5	63.6	88.5	107.3	121.5
μ (thick)	5.82×10^{-7}	4.74x	4.58x	4.45x	4.25x
μ (thin)	2.67x	2.17x	2.10x	2.04x	1.95x

VII. TEST TRANSMISSION

ENGINEERING, DESIGN, AND MANUFACTURE

A. DISCUSSION

The basic design requirements of the subject transmission are as follows:

1. Input Speed - 30,000 R.P.M.
2. Input Power - 250 Horsepower
3. Ratio - 85:1

Due to the unique character of harmonic drive, the required ratio can be most readily accomplished in a single stage. While this produces a simple unit, it means that the input speed and the output torque are closely connected rather than separated by several stages as in conventional reduction units. This imposes the requirement that diameters be minimized while torque capacity is maintained at a high level. A recent development in flexspline design has made it possible to produce flexsplines with longer than normal tooth lengths, thus achieving load-carrying capacity by use of length rather than diameter.

To compensate for the torsional windup of the flexspline under full load, the teeth of the flexspline were made with a slight helix. The major area of study is the wave generator bearing. This bearing must be capable of properly supporting the loads and shape of the flexspline while rotating at input speed. The wave generator surface is contoured to produce the necessary converging wedge-shaped oil film to provide the pressure profile needed by the flexspline. Certain broad assumptions were made based upon the best available data. After determing the required pressure profile, a trial and error approach using graphic integration of the Reynold's equation was used to determine the contour.

Barriers were placed on the ends of the wave generator to minimize end leakage. During testing, these raised barriers experienced overload. The barriers were removed. Any subsequent end leakage which may have occurred had no

noticeable effect. A relief is provided in the unloaded zone of the wave generator to reduce losses and facilitate the introduction of lubricant.

Difficulties were encountered in cutting the spline teeth. The problem was caused by the large number (510) of extremely fine (96 diametral pitch) teeth of long length (6 inches). Future units could be designed with 340 teeth of 64 diametral pitch; this would ease the manufacturing problem greatly.

DESIGN CALCULATIONS

Stated input to reducer: 250 horsepower at 30,000 r.p.m.

Helicopter design criteria provided by Kaman Aircraft Corporation:

Output Torque - Ultimate - 120,000 inch-pounds
Limit - 80,000 inch-pounds
Design - 40,000 inch-pounds

Life - 300 hours at 40,000 inch-pounds
450 hours at 24,600 inch-pounds
250 hours at 22,200 inch-pounds
1,000 hours total

Basic Working Dimensions: (supporting calculations are presented later in this analysis)

Circular Spline Pitch Diameter	5.3750	Inches
Tooth Length	5.00	Inches
Flexspline Pitch Diameter	5.3125	Inches
Flexspline Bed Thickness	0.1105	Inches
Flexspline Inside Diameter	5.0625	Inches
Flexspline Overhang At Each End	.50	Inch
Wave Generator Total Length	6.00	Inches
Wave Generator Working Diameter, Average	5.06	Inches
Reduction Ratio	85:1	

Pitch Diameter of Circular Spline:

$T = KD^3$, from harmonic drive design standards

let K = 250, an assumption based on past experience

$T = 250\ D^3$

$40{,}000 = 250\ D^3$

D = 5.42 inches approximately

Diametral Pitch (P_D) = 96, selected

Tooth Difference (Nd) = 6, selected

$R = \frac{No}{Nd}$, from harmonic drive design standards

$85 = \frac{No}{6}$

No = 510

Nf = No $\pm$Nd, by definition

= 510 + 6

= 516

Dpc = Nf/P_D, by definition

= 516/96

= 5.3750 inches actual

Pitch Diameter of Flexspline:

Dpf = No/P_D, by definition

= 510/96

= 5.3125 inches actual

Flexspline Dimensions in Inches:

Pitch Diameter = 5.3125

Dedendum = .0145

Root Diameter 5.3125 -2x.0145 = 5.2835

Inside Diameter = 5.0625

Bed Thickness (5.2835 -5.0625)/2 = .1105

Mean Bed Diameter 5.0625 + .1105 = 5.173

Mean Bed Radius 5.173/2 = 2.586

Flexspline Deflection (d):

d = Dpc -Dpf, by definition

= 5.3750 -5.3125

= .0625 inch

This means that each tooth moves outward .0312 inch from its circular shape at each major axis and inward a little less than this at the minor diameter.

Flexspline Deflection Stress:

$$Sf = \frac{3Edt}{D^2}, \text{ from harmonic drive design standards,}$$

$$= \frac{3x30x10^6x.0625x.1105}{5.173^2}$$

= 23,200 p.s.i.

Flexspline Load Stress:

$$St = \frac{T}{DAr}, \text{ from harmonic drive design standards,}$$

$$= \frac{40,000}{5.17x5x.1105}$$

= 14,000 p.s.i. at design torque

Flexspline Tooth Shear Stress:

$$Ss = \frac{T}{0.1D^2L}, \text{ from harmonic drive design standards,}$$

$$= \frac{40,000}{0.1x5.3125^2x5}$$

= 2830 p.s.i. at design torque

Flexspline Bell Face Shear Stress:

$$Ss = \frac{T}{RA}, \quad A = 2 \pi Rt$$

$$= \frac{40,000}{2.6x2\pi x2.6x.08}$$

= 11,800 p.s.i. at design torque

Flexspline Torsion Stress:

$$Ss = \frac{2Tr_1}{\pi(r_1^4 - r_o^4)}, \text{ Reference 3, P175}$$

$$= \frac{2x40,000x2.639}{\pi\ (2.639^4 - 2.531^4)}$$

= 9000 p.s.i. at design torque

Torsional Deflection of Flexspline:

This is the torsional deflection that will occur in the length of the teeth with a distributed load shared by all the teeth throughout their length.

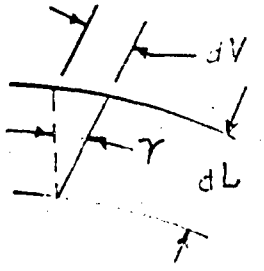

$$\gamma = \frac{dV}{dL}, \text{ by definition} \qquad (1)$$

$$\gamma = r \qquad (2)$$

$$\theta = \frac{TL}{GI_p} \qquad (3)$$

Combining Equations (1), (2), and (3):

$$\frac{dV}{dL} = \frac{rTL}{GI_p} \qquad (4)$$

Integrating:

$$V = \frac{rTL^2}{2GI_p} + C \qquad (5)$$

Evaluating for C and substituting into Equation (5):

$$V = \frac{rT}{2GI_p}(L^2 - 25) \qquad (6)$$

$$= \frac{2.586 \times \frac{40,000}{5}}{2 \times 12 \times 10^6 \times 2\pi \times 2.586^3 \times .1105}(0^2 - 25)$$

$$= .0018 \text{ inch}$$

That is, the maximum twist is .0018 inch in 5 inches or an average twist of approximately .0004 inch/inch.

Wave generator design (for this section, a torque of 31,200 inch-pounds is assumed as a design value lying between the various operating torques).

Flexspline Deflection Force:

$$F = \frac{.56dLt^3E}{r^3}, \text{ from harmonic drive design standards,}$$

$$= \frac{.56 \times .0625 \times 6 \times .1105^3 \times 30 \times 10^6}{2.586^3}$$

$$= 401 \text{ pounds}$$

$$\text{Or } \frac{491}{6} = 81.8 \text{ pounds/inch}$$

Since the bell shape has been found to add very little stiffness to short splines, it is assumed that it adds nothing to the long spline.

Note that the above force is calculated as if the flexspline were deflected by forces concentrated along a line at the major axis. The actual flexspline will be supported by oil pressure which may be assumed to be distributed over an arc of 30 degrees before the major axis and 15 degrees behind it.

Length of supporting arc:

$$L = \pi D \frac{\alpha}{360}$$

$$= \pi \times 5.06 \times \frac{45}{360}$$

$$= 1.987 \text{ inches}$$

Average pressure:

$$P_{ave} = \frac{F}{A}$$

$$= \frac{81.8}{1.987 \times 1}$$

$$= 41.2 \text{ p.s.i.}$$

Since the distributed pressure could be somewhat greater from a concentrated force, a pressure of 50 p.s.i. is assumed.

Maximum Pressure:

$P_{max} = P_{ave} \times \frac{\pi}{2}$, assuming a sinusoidal pressure distribution

$= 50 \quad \frac{\pi}{2}$

$= 78.5$ p.s.i.

Or 80 p.s.i.

Tooth Separating Forces:

$F = \frac{T}{D} \tan \alpha$ from harmonic drive design standards

$= \frac{31,200}{5.375} \tan 14\text{-}1/2$ degrees

$= 1503$ pounds

Or $\frac{1503}{5} = 301$ pounds per inch

Pressure To Support Separating Load:

Assume that the separating load of 301 pounds is distributed over 30 degrees of arc, symmetrical with the major axis, and with a sinusoidal pressure distribution.

Length of Supporting Arc:

$L = \pi D \quad \frac{\alpha}{360}$

$= \pi \; 5.06 \times \frac{30}{360}$

$= 1.325$ inches

Average Pressure:

$$P_{ave} = \frac{F}{A}$$

$$= \frac{301}{1.325 \times 1}$$

$$= 227 \text{ p.s.i.}$$

Maximum Pressure:

$$P_{max} = P_{ave} \frac{\pi}{2}$$

$$= 227 \frac{\pi}{2}$$

$$= 357 \text{ p.s.i.}$$

Pressure profile to develop output torque.

It is believed that a pressure profile in which

$$P = K \phi$$

from the minor axis ($\phi = 0$) to the major axis ($\phi = \pi/2$) will maintain the flexspline in position and develop necessary force to produce the output torque. It can be shown that the moment arm of a force acting normally to a harmonic drive wave generator surface is as follows:

$$La = \frac{2d}{D} r \sin 2\phi .$$

By multiplying the pressure on a point by the area of that point ($rLd\phi$), the force on that point can be obtained. When this is combined with the moment arm of that point and summed with all the other points, the torque on the input shaft which is transferred to useful output is obtained.

Thus:

$$T = 2 \int_0^{\pi/2} \frac{2d}{D} r \sin 2\phi \times K \phi \, rLd \phi$$

and

$R = \frac{D}{d}$, from harmonic drive design standards; combining, simplifying, and integrating:

$$T = Kr^2 L \pi$$

$$31,200 = K \times 2.53^2 \times 5 \times \pi$$

$$K = 310 \text{ p.s.i.}$$

Pressure at Major Axis:

$$P = K \phi$$

$$= 310 \times \frac{\pi}{2}$$

$$= 487 \text{ p.s.i.}$$

Oil Film Profile Calculations:

Observing the total required pressure curve (IV) of Figure 18, it is required to develop an oil film profile which will generate the pressure profile. Refer to Shaw and Macks "Analysis and Lubrication of Bearings", Reference 4, Page 332.

This section outlines a technique for determing the pressure profile that will be generated by an oil film profile under a given set of viscosity-velocity conditions. The technique consists of assuming a likely looking oil film profile, selecting a viscosity, and then calculating the pressure profile as outlined in the text. The calculated pressure curve will not be correct on the first try. Subsequent modifications of the oil film profile will, after a number of trials, lead to the desired pressure profile.

This procedure was followed through a number of trials, ending with the final set of calculations which follow. The pressure curve is plotted as Calculated Pressure Curve V of Figure 15, and the oil film profile is plotted on the upper half of Figure 15.

$$P = \int_o^x \frac{6 \mu UB}{h^2} dx - C_1 \int_o^x \frac{6 \mu UB}{h^3} dx$$

and

$$C_1 = \frac{\int_0^x \frac{6\mu UB}{h^2}dx \Big|_{x=1}}{\int_0^x \frac{6\mu UB}{h^3}dx \Big|_{x=1}}$$

$$P = \int_0^x \frac{6x2x10^{-7} x \frac{30.000x5.0625\pi}{60} x 5.0625\pi \frac{105}{360} x \frac{5}{105}}{h^2}$$

$$-C_1 \int_0^x \frac{6x2x10^{-7} x \frac{30.000x5.0625\pi}{60} x 5.0625\pi \frac{105}{360} x \frac{5}{105}}{h^3}$$

$$P = \int_0^x \frac{212x10^{-5}}{h^2} \quad -C_1 \int_0^x \frac{212x10^{-5}}{h^3}$$

Applying the graphic integration technique to the above expression produces the following table of numbers, in which Column "G" gives the pressure (P).

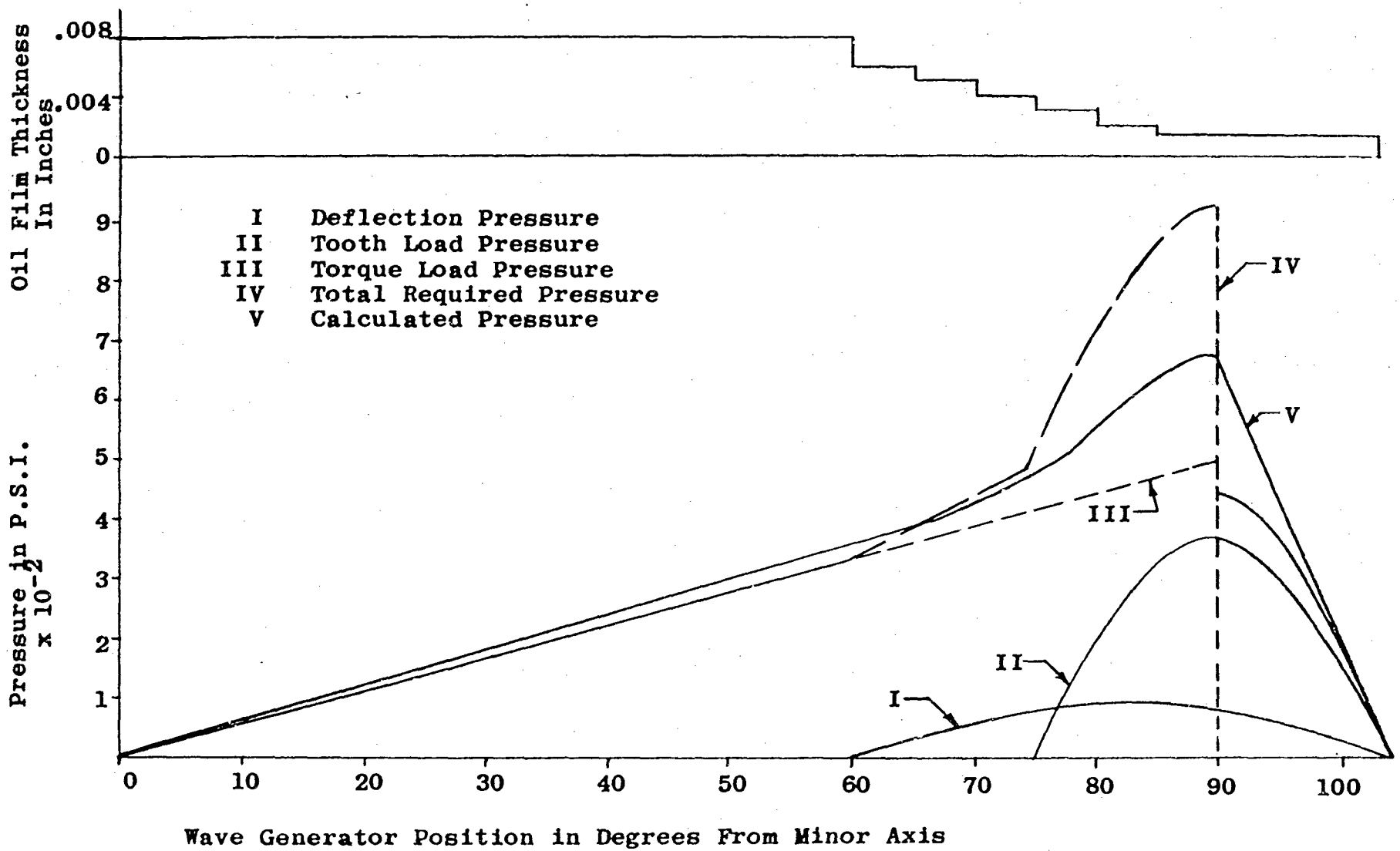

Figure 15. Wave Generator Pressure Distribution

TABLE II

CALCULATED PRESSURE, CURVE V, FIGURE 15

Station	h	h^2	h^3	"A" $\frac{212.12 \times 10^{-5}}{h^2}$	"B" $\frac{}{h^3}$
0^o	∞	∞	∞	0	0
5	$7.5x\ 10^{-3}$	$56.25x\ 10^{-6}$	$421.77x\ 10^{-9}$	37.71	$5.029\ 10^3$
10					
15					
20					
25					
30					
35					
40					
45					
50					
55					
60					
65	7x	49x	343x	43.29	6.184x
70	6x	36x	216x	58.92	9.820
75	5x	25x	125x	84.85	16.970
80	4x	16x	64x	132.57	33.144
85	3x	9x	27x	235.69	78.563
90	2x	4x	8x	530.30	265.15
95	1.5x	2.25x	3.37x	942.76	629.44x
100	1.5x	2.25x	3.37x	942.76	629.44x
105	1.5x	2.25x	3.37x	942.76	629.44x

Station	"C" $\int$ "A"	"D" $\int$ "B"	"E" $\frac{\text{"C105"}}{\text{"D105"}}$	"F" "D"x"E"	"G" "C"-"F"
0^{o}	0	0		0	0
5	37.71	5.029 $x10^{3}$		9.31	28
10	75	10x		19	56
15	113	15x		28	85
20	151	20x		37	114
25	189	25x		47	142
30	226	30x		56	170
35	264	35x		65	199
40	302	40x		74	228
45	339	45x		84	256
50	377	50x		93	284
55	415	55x		102	313
60	453	60x		112	341
65	496	67x		124	372
70	555	77x		143	412
75	639	93x		172	467
80	772	126x		233	539
85	1008	205x		380	628
90	1538	470x		870	668
95	2481	1100x		2037	444
100	3424	1729x		3201	223
105	4366	2358x	1.8516x 10^{-3}	4366	0

Flexspline Harmonic Shape:

Outward delfection at major axis = .03125 inch. Inward deflection at minor axis, Reference 3, page 156

$\frac{137}{149}$ x .03125 = .02875 inch.

Total deflection .03125 + .02875 = .060 inch.

$$r_{\phi} = r_{\phi = 0} + \frac{d}{2}(1 - \cos 2\phi)$$, this is harmonic or sine wave shape

$$r_{\phi = 0} = 2.53125 - .02875$$

$$= 2.5025 \text{ inches}$$

$$r_{\phi} = 2.5025 + \frac{.060}{2}(1 - \cos 2\phi)$$

This formula was solved for every degree from $\phi = 0$ to $\phi = 180$ degrees.

Wave Generator Profile Calculations:

Radius Wave Generator = Radius Flexspline -h

Oil Barrier Profile:

Since the oil film thickness was calculated to be .0075 from 0 degrees to 60 degrees, it was considered desirable to raise "barriers" at the ends of the wave generator to reduce end leakage and to maintain a reasonably uniform oil pressure over the full length of the spline teeth. These barriers were removed during testing after experiencing overload. Any subsequent end leakage which may have occurred had no noticeable effect. It was considered desirable that this barrier have an oil film thickness equal to the minimum of the wave generator (.0015 inch). At accidental low loads, the major diameter of the flexspline might increase to .005 inch or .0025 inch on the radius and the minor diameter decrease by the same amount. To be safe, the wave generator is proportioned for nominal oil film thickness at the minor diameter of .004 inch and

at the major diameter of .0015 inch.

$$r_{\phi} = 2.5025 - .0040 + \frac{.060 + .0025}{2} (1 - \cos 2\phi)$$

Oil Exchange Area:

The oil exchange area was designed as a pocket for the following reasons:

1. To keep the pressure low and uniform as the oil enters the wedge.

2. To provide a generous mixing area so that hot oil will be evenly diluted with cool oil before entering the wedge.

3. To provide small exit areas so that air will not enter and start foaming in the exchange area.

The exchange area is cut to an approximately equal depth throughout. The exchange area barriers are designed with a film thickness of .02 inch.

$$r_{\phi} = 2.5025 - .020 + \frac{.060}{2} (1 - \cos 2\phi)$$

Since this area would be difficult to cut as a cam, it was designed to be formed as a series of cuts with 5-degree spacings, using every fifth point.

Hydrodynamic efficiency of wave generator hydrodynamic bearing,

$$F = \frac{\mu \, UBL}{h_2 \left(\frac{h_1}{h_2} - 1\right)} \left[4 \ln \frac{(h_1)}{h_2} - 6 \frac{\left(\frac{h_1}{h_2} - 1\right)}{\left(\frac{h_1}{h_2} + 1\right)} \right]$$

From Reference 4, page 326.

Since this formula is for a wedge with constant taper from h_1 to h_2, it is necessary to make some corrections to h_1.

Average Oil Film Thickness:

$$h_{ave} = \frac{.0075 \times 60 + \frac{.0075 + .0015}{2} \times 35 + .0015 \times 10}{105}$$

$$= .00592 \text{ inch}$$

Corrected Maximum Film Thickness:

$$h_1 = 2\, h_{ave} - h_2$$

$$h_1 = (2 \times .00592) - .0015$$

$$= .01034 \text{ inch}$$

$$F = \frac{2 \times 10^{-7} \times \frac{30000 \times 5.0625\pi \times 5.0625\pi}{60} \times \frac{105}{360} \times 6.00}{.0015 \left(\frac{.01034}{.0015} - 1\right) \left[4 \ln \left(\frac{.01034}{.0015}\right) - 6 \frac{\left(\frac{.01034}{.0015} - 1\right)}{\left(\frac{.01034}{.0015} + 1\right)} \right]}$$

$$= 16.24 \text{ pounds on one axis}$$

Or 32.48 pounds total

$$T = Fr$$

$$= 32.48 \times 2.5312$$

$$= 82.2 \text{ inch-pounds}$$

$$p = \frac{TN}{63,000}$$

$$= \frac{82.2 \times 30,000}{63,000}$$

$$= 39.2 \text{ horsepower}$$

$$e = \frac{250 - 39.2}{250}$$

$$= 84.3 \text{ percent assuming laminar flow, hydrodynamic bearing losses only}$$

This prediction, based on test unit proportions, agrees quite well with the 83 percent prediction of the parametric analysis, Figure 14, page 32.

VIII. TEST PROGRAM AND EVALUATION

A. STARTING TORQUE

The deflected flexspline imposes a static line-contact load on the wave generator at the major axis. On the test transmission, this load was calculated to be 491 pounds (Section VII). Starting torque must overcome the friction resulting from this load under conditions of essentially metal-to-metal contact. The situation is presented in greater detail in the Appendix, as is a discussion of theory and experimentation undertaken to reduce starting torque and possibly improve hydrodynamic bearing operation.

Briefly, appropriate nondirectional pocketed surfaces were found to be effective in improving boundary layer lubrication characteristics. The theory and experiments indicated that starting torque could be reduced by this method. In addition, this treatment could allow hydrodynamic bearing operation to approach the incipient boundary layer zone where efficiency is greatest. The hydrodynamic bearing was established by test to be able to support 61 percent more load than the calculated capacity. This surface finish treatment may have contributed to this performance.

Starting torque under various circumstances is reported in the following graph, Figure 16. The transmission, as received, was disassembled. The wave generator surface finish was RMS 16-20, circumferentially ground. The flexspline had a highly polished mirror finish. The flexspline was mounted in a test fixture, deflected with clamps, the wave generator inserted, and the clamps released. Starting torque in pound-feet was measured with MIL-O-6081-1010 turbine engine oil as the lubricant. This is reported in Column 1. The lowest value was 54 pound-feet; the highest was 84 pound-feet; the most common value was 66 pound-feet. Starting torque was observed to be sensitive to position and time lapse. The parts were glass bead peened to 15-20 RMS on the wave generator and 35 to 45 RMS on the flexspline. The starting torque test was then repeated with a low value of 30 pound-feet, a high of 54 pound-feet and a most common value of 42 pound-feet. This is reported in Column 2.

The test was repeated with the break-in lubricant, Ore Lube K-40, which contains a colloidal suspension of molybdenum disulfide particles. The low, high, and most common values were 24, 60, and 42 pound-feet respectively (Column 3).

A hardened wave generator surface requirement had been anticipated, but was dependent on establishing that a suitable contour existed on the wave generator surface. Initial testing established the contour as operationally satisfactory. With further testing, the surface deteriorated from hydrodynamic erosion, establishing that the anticipated hardening was required before further testing could continue. This hardening took the form of electroless nickel plate .0004 inch thick. The plate hardness after heat treat was Rockwell C-60 (converted), considered adequate to prevent further erosion.

Four parameters were changed by the plating: (1) The nickel plate did not precisely reproduce the pocketed surface obtained by glass bead peening, which could increase friction; (2 and 3) The nickel surface provided differential hardness and differential materials in contact because the flexspline (steel) was not changed, which should reduce friction; (4) The plating increased the wave generator dimensions, requiring greater flexspline deflection, resulting in increased load which would increase friction.

Starting torque with MIL-O-6081-1010 oil ranged between 40 and 50 pound-feet with no most common value (Column 4). The wave generator was hand-polished on both major axis lines of contact with gamma aluminum oxide to remove any possible protuberances from the plating process. This had no noticeable effect. The unit was then tested with Molykote G, which contains molybdenum disulfide, again with no noticeable effect (Column 5). It was concluded that the reduction in starting friction obtained with glass bead peening was not appreciably altered by nickel plate. The independent effects of the four variables are not known. Compensating effects may be present. The scatter was considerably reduced.

Column 6 shows the values which the data in the Appendix indicate could be achieved with all parameters optimized, 30 to 39 pound-feet. Because of the many process variables, as well as possible errors in assumptions of load distribution, this optimum was not reached.

Column 7 shows the values which could be expected for an improved transmission. The rework investigated includes shortening the flexspline from 6 inches to 3.25 inches and decreasing the bed thickness from .1105 inch to .086 inch. The deflection force is then:

$$F = \frac{.56\ d\ L\ t^3 E}{r^3}$$ from harmonic drive standards

where:

d = .0625 (unchanged)

L = 3.25 inches

t = .086 inch

E = 30×10^6 (unchanged)

r = mean bed radius = 1/2 (root diamter -t) =

$$\frac{5.2835-086}{2} = 2.59875 = 2.60$$

then:

$$F = \frac{(.56)(.0625)(3.25)(.086)^3(30)(10^6)}{(2.60)^3} = 123.5 \text{ pounds}$$

or: $\frac{123.5}{3}$ = 41 pounds per inch.

The previous load (calculated) was 81.8 pounds per inch. The starting torque may therefore be expected to be cut in half. This ratio was used for the prediction of starting torque for the reworked transmission.

In addition, the wave generator would be hardened. A program similar to that reported in the Appendix could determine the optimum combination of pocketed non-directional surfaces with differential hardness for the reduced load. The prediction in Column 7 may be conservative in that no reduction is predicted on improvement from such a program.

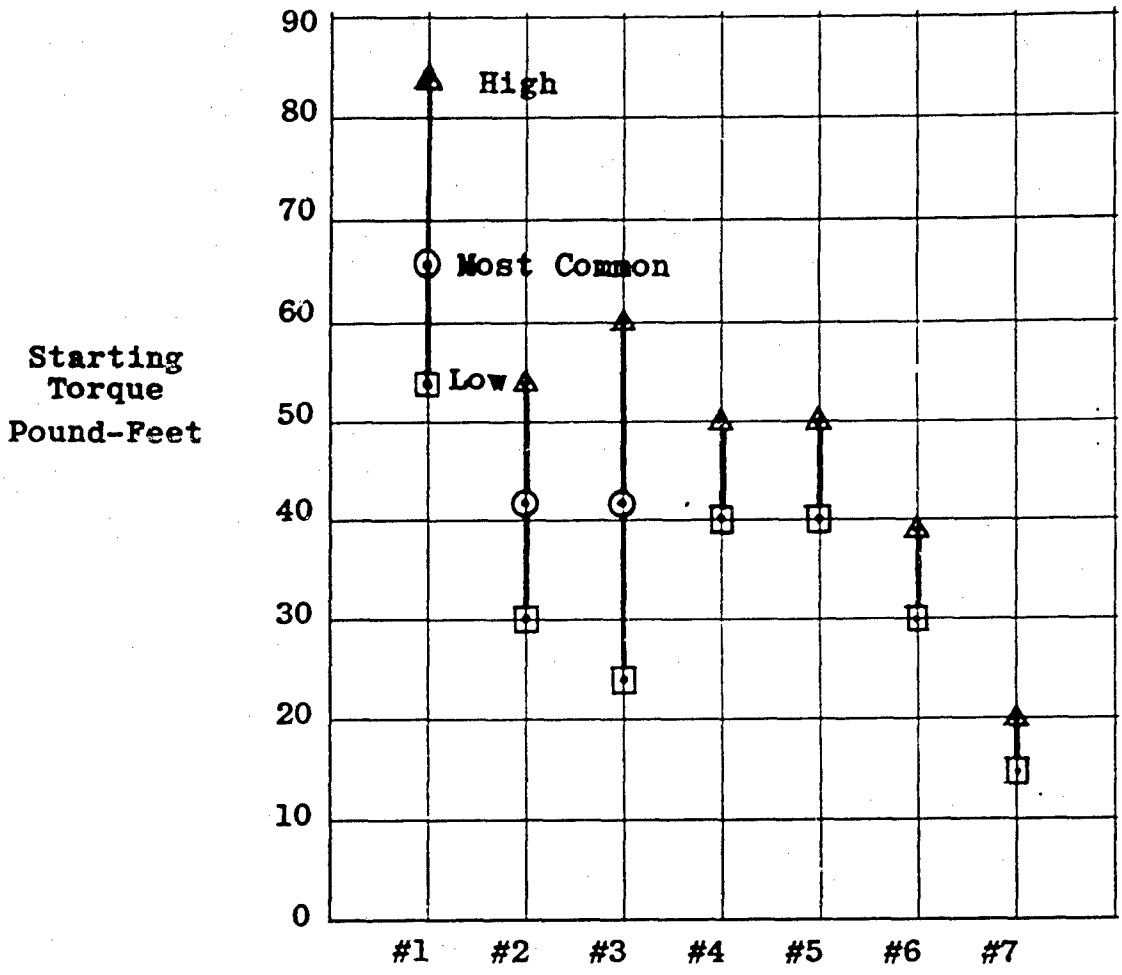

Figure 16. Starting Torque Characteristics

Summary of Test Conditions:

1 Wave Generator - 16-20 RMS, Circumferentially Ground
Flexspline - Polished Mirror Finish
Lubricant - MIL-O-6081-1010 Oil

2 Wave Generator 15-20 RMS, Glass Bead Peened (.007 inch diameter)
Flexspline 35-45 RMS, Glass Bead Peened (.020 inch diameter)
Lubricant - MIL-O-6081-1010 Oil

3 Same As 2 Except Lubricant - Ore Lube K-40 Oil
(Molybdenum Disulfide Additive)

4 Wave Generator - .0004 Nickel Plate, Hardened to RC-60
Flexspline - Unchanged; Lubricant - MIL-O-6081-1010 Oil

5 Same As 4 Except Lubricant - Molykote G Grease
(Molybdenum Disulfide Additive)

6 Possible Per Test Data, All Parameters Optimized (See Appendix)

7 Predicted For Improved Transmission, Based On Flexspline Shortening And Thinning

B. EFFICIENCY INVESTIGATION

1. Introduction

Purpose - The Analysis of Problem, Section VI, established operating efficiency as the essential area of investigation. This focused attention on the hydrodynamic bearing characteristics of the wave generator/flexspline interface. The bearing is unconventional because of its load distribution and flexibility. The test program was directed toward exploring the operating characteristics and efficiency improvement possibilities of this bearing.

Method - Test planning was based on the assumption that the performance of the hydrodynamic bearing can be defined in terms of the parameter ZN/P where Z is viscosity in centipoises, N is r.p.m., and P is pressure. This assumption is commonly used in sliding bearing technology. Analytical justification may be found in the literature. This approach is most useful to test programs, because it allows expensive and dangerous parameters (speed and load) to be reduced to manageable values with the added freedom of simulation by viscosity control. The design values for this hydrodynamic bearing are Z = 0.6 centipoise (JP-4), 30,000 r.p.m., and 100 percent input torque (525 pound-inches). This could be simulated at Z = 6 centipoises (MIL-O-6081-1010 turbine engine oil), 3,000 r.p.m., and 100 percent input torque. This represents a considerable reduction in the expense and danger involved in testing. The validity of a 10 to 1 extrapolation is, of course, open to question. The ultimate answer to this question is full-scale testing.

The results of this test program are discussed with respect to the following goals under Test Program Conclusions, page 72.

Goals:

a. Establish ZN/P as a suitable parameter for efficiency testing for this bearing.

b. Determine the practical limit of viscosity reduction as a method of improving efficiency.

c. Investigate turbulence as a limiting factor.

d. Observe the operating characteristics of this bearing as a novel hydrodynamic bearing approach.

e. Observe the operating characteristics of the harmonic drive test transmission.

f. Predict expected efficiency of harmonic drives with hydrodynamic bearings through scale testing for the power spectrum of the parametric analysis.

2. Test Apparatus

Drive Train - The drive train (in series) consisted of a 100-horsepower electric motor prime mover, a Gyrol variable speed drive (input speed control), a 5 to 1 speed-up timing belt drive to the input drive shaft, a rubber flexible coupling, the test transmission, a chain-type flexible coupling connecting the transmission to the output drive shaft, and an adjustable servo-controlled prony brake (output torque control).

Lubrication System - A 15-gallon oil tank contained a visible sight gage, a breather, a magnetic chip collector, and a temperature controllable immersion heater for preheating the oil. Next was a 50-p.s.i. pressure pump, a filter, two flow meters in parallel with a shut-off valve for one, through a rotary seal, and the output drive train to the test transmission. The wave generator contained an oil gallery in its axle. Radial holes fed oil to the various transmission bearings. Five parallel radial holes fed oil to each of the two unloaded quadrants of the wave generator. These holes were choked by means of two indexed replaceable rods which intersected the parallel radial holes. These rods were close to the surface of the wave generator. The replaceable rods metered oil to the wave generator bearing by restricting flow through small orifices drilled through the rods in line with the parallel radial holes. The orifice size which was found to be satisfactory was .040 inch, resulting in a flow of 4 gallons per minute and an acceptable temperature rise. After passing through the hydrodynamic bearing, the oil was collected by drains and scavenged from the output end of the transmission housing. This allowed partial flow

between the flexspline teeth and the circular spline teeth. The oil trapped between these teeth was pumped to the scavenging sump by the flexspline rotating tooth mesh. Helical grooves in the circular spline teeth controlled the direction of this flow. Forward scavenging provisions were provided to relieve excess pumping if it occurred. Excess pumping did occur at high speeds, but the forward provisions were not used, because of the danger of supplying too little oil to the tooth mesh at the lower speeds, the area of greatest interest. Controlled oil supply to this mesh would eliminate the power loss caused by the scavenged oil pumping. From the sump, a scavenge pump returned the oil through a convection cooler to the tank. The convection cooler was arranged to permit muffling for increasing oil temperature or fan cooling for decreasing oil temperature.

Instrumentation - Input speed was read by a tachometer on the input drive shaft. A stroboscope monitoring input torque also provided input speed values. The input speed was recorded by a timing track on the oscillograph record.

Input torque was measured by a strain gage rosette mounted on the input drive shaft adjacent to the transmission input coupling. Two bridges were installed and each calibrated for strain versus torque. The signals were lead through slip rings to a visible gage. Redundancy was thus provided. In addition, the input drive shaft consisted of an outer tube which rotated but carried no torque, and an inner tube which rotated and carried torque. The tubes carried circular plates located at the transmission input end of the input drive shaft. These plates were circumferentially marked so that differential torsional deflection could be read as input torque by stroboscope. The purpose of this arrangement was to provide a mechanical system to supplement the electrical system. One electrical failure did occur, the strain gages were unable to indicate torque higher than 50 percent, and the mechanical torquemeter system did prevent overload.

Output torque was measured by a pneumatic servo-controlled, water-cooled prony brake. The brake operated against a calibrated spring scale. Deflection of the scale opened or closed a valve monitoring air pressure to a pneumatic actuator which applied tension to a brake band on the brake drum. This system hunted approximately $\pm$1 percent.

Oil flow was monitored by two flow meters. These could be read in parallel and summed, then one shutoff for a single flow meter reading. The purpose was to provide a fail-safe method of monitoring oil supply. No discrepancies were observed.

Inlet oil temperature was measured by a thermocouple mounted within the stationary element of the rotary oil seal, immediately before the oil entered the transmission.

Outlet oil temperature was measured by a thermocouple mounted in an internal housing cavity immediately adjacent to the wave generator bearing. This cavity received heated oil as it left the hydrodynamic bearing.

Oil film thickness was measured by capacitance change with flexspline radial displacement. Insulated probes were mounted in radial holes through the housing. These probes were threaded for radial adjustment and calibration. With the major axis of the wave generator directly under the probe, the probes were adjusted inward to make contact with the flexspline. They were then retracted and capacitance value recorded for increments of .001 inch for a .005-inch gap. During operation, the oil film between the wave generator and the flexspline caused the flexspline to be displaced radially outward toward the probe as the major axis passed. This deflection was read by comparing capacitance value with the calibration curve for that probe. The distance thus found, subtracted from the retracted distance, gave the oil film thickness. In actual practice, the calibration scale was inverted on the oscilloscope to permit direct reading of oil film thickness. Traces recorded on the oscillograph during testing preserved oil film thickness measurements. There

were five axial probes to measure longitudinal film thickness distribution. At each end of the row of axial probes, an additional probe was circumferentially displaced 90 degrees to determine if skewing was present. Thus, there were seven probes in all.

This method of film thickness measurement was not entirely satisfactory for two reasons: chiefly, probe calibration proved to be a lengthy, time-consuming process; the second drawback was that distance versus capacitance is a hyperbolic scale. The area of greatest interest, the minimum film thickness associated with highest efficiency, was the most difficult to read. The capacitance varied from .03 inch scale for a .001-inch oil film to 0.3 inch scale for a .005-inch oil film. This was overcome by using the threaded mount for the probe as an improvised micrometer, running the probe in until contact was reached, followed by retracting the probe to its initial position.

3. Tests

The initial tests were with a high-viscosity lubricant, Ore Lube K-40. The viscosity was measured to be Z = 140 centipoises at 100 degrees F., which required a scale speed of 129 r.p.m. at full torque to be equivalent to design conditions. Testing with K-40 was followed by testing with a much lower viscosity oil. This was desired to investigate the validity of the ZN/P parameter over as wide a range of variables as possible. In addition, K-40 contains a colloidal suspension of molybdenum disulfide particles, which was considered desirable for its use as a break-in lubricant.

A no-torque run of 32 minutes at less than 100 r.p.m. was used to checkout the power and drive train, oil system, and internal oil distribution and to permit the accumulation of filtrate sludge which could contain wear particles. Two probes were removed from the housing for visual observation of tooth action and oil flow. The transmission was found to be exceedingly quiet. The spline teeth had a through oil flow as planned, although larger than expected. The situation appeared not to require the connection of the scavenge provisions which

would have reduced this flow. The filtrate sludge was analyzed and found to contain paint, sand, unidentified foreign objects, and some ferrous particles. The ferrous particles were of two types characteristically found in all new transmission sludge: flat flakes and irregularly shaped particles which could be "fuzz" or wear. The flakes are believed to be from shims and rapidly cease appearing. The ferrous dust is of more interest. The only part containing nickel was the flexspline (SAE 4340). It was also the part most likely to show wear. The ferrous residue was therefore tested for nickel content. The test is quite positive and quite sensitive. No evidence of nickel was found. The conclusion was that flexspline wear was not occurring and the test transmission integrity was sufficient to begin testing.

The transmission was then tested with the high-viscosity lubricant. The results are shown on Figure 20, A1 through A4. The data are summarized in Table III. Difficulty was encountered in maintaining the low speed required. Gyrol overheating limited testing. Sufficient data were recorded to provide the wide range of ZN/P desired and to overlap the ZN/P values expected with the low-viscosity lubricant.

The high losses associated with turbulence were not observed. The oil film thickness was found to be more sensitive to speed than to load by a large ratio. With this lubricant, the effect of 25 percent, 50 percent, 75 percent, and 100 percent design input torque was effectively negligible in that the film thickness variation was less than the probes could measure with certainty while changes in r.p.m. caused easily measured changes. The oil film was consistently thicker than .005 inch, when .002 inch would be ample. This test series was therefore concluded. Lubricant viscosity measured after testing was found to be 108 centipoises at 100 degrees F.; possibly this was the result of oil filtration. The viscosity curve measured after testing was used for the ZN/P values shown on Figure 17. Z (viscosity) varied from 95 to 110 centipoises; N (speed), from 382 r.p.m. to 439 r.p.m.; and P (pressure), expressed in terms of percent Ti (input torque), from 55 to 100. After several preliminary runs, a total of four cases were recorded from two separate runs. ZN/%Ti varied from 367 to 764.

The low viscosity lubricant tests were with MIL-O-6081-1010. With this oil, Z = 6 centipoises at 120 degrees F., requiring a scale speed of 3,000 r.p.m. at full torque to be equivalent to design conditions. The cleanliness requirement was apparently violated. On the initial run with this oil, the test unit was damaged by a foreign particle which was larger than .005 inch (oil film thickness) and smaller than .040 inch (oil jet diameter). A furrow was ploughed on the wave generator loaded quandrant immediately adjacent to the dam (end leakage barrier) on the output end. This resulted in scoring of both the wave generator and flexspline surfaces. The wave generator was reworked to remove the dam and the damaged area to below contour. The flexspline was locally polished.

Testing was resumed. The purpose of the dam had been to reduce end leakage. Removal of the dam proved to have a negligible effect on measured major axis film thickness. After a limited test (not reported), damage was again sustained by the wave generator and flexspline. Part of the damage occurred in a manner and at a location not accounted for by theory. This necessitated an investigation into the cause and corrective action required. Briefly, the minor axis of the wave generator, dam area, input end was found to be a well-lubricanted, extremely overloaded zone of distress. The wave generator dam surface was stretched in the direction of rotation to such an extent that transverse cracks appeared. The edges of the cracks crumbled progressively upstream. The major axis, output end, sustained scoring which was caused by metal pick-up, local welding, and tearing.

A static load investigation was conducted to explore this possible source of the unpredicted load on the minor axis. Clearance was established at the minor axis by feeler gauge measurement, and the only known static load, input torque, was applied with the output shaft locked. There was no measurable change in the minor axis clearance.

A vibratory load investigation was conducted which consisted of (1) impact tests on the wave generator and flexspline to find component mode shapes and frequencies and (2) a shake test to determine system deformations. The deflected shape of the flexspline is, of course, the first harmonic wave shape of a bell mode vibration, while the power input end is the location of greatest amplitude for a cantilever mode vibration. No information was found to indicate that wave generator minor axis distress was a resonance problem.

Hydrodynamic consideration of the nature of the distress and the geometry of the components led to recommendations for corrective action. These included increased surface hardness to overcome effects of possible cavitation and removal of sharp corners from the inlet and exit edges of the loaded quadrant surfaces to reduce high local pressure gradients in the lubricant film. These edges showed hydrodynamic polishing with no metal contact indicated.

Increasing the hardness of the cam surface could be expected to eliminate major axis scoring and the damage caused by cavitation. It might also reduce starting torque. In addition, less abrupt transitions in the lubricant flow path were felt to be desirable. The minor axis distress, dam area, input end, was felt to be largely the result of the presence of the dam. The oil film thickness was measured as .005 inch at the major axis. Because the circumference of the flexspline must remain approximately constant, increase in clearance at the major axis could be accompanied by a corresponding decrease in clearance at the minor axis. Thus, an extremely thin oil film, implying high local pressure, could be expected on the dam at the minor axis. To correct this condition, this dam was also removed to below contour. The scored area on the major axis, output end, was also removed to below contour, and the flexspline was locally polished. These changes reduced the length of the load bearing quadrants on the wave generator from 6 inches to 4-3/4 inches. The inlet and exit edges on the load bearing quadrants were hand-stoned. The load bearing surfaces were then electroless nickel plated, .0004 inch thick.

The plate hardness after heat treat was Rockwell C-60 (converted), considered adequate. The major axis lines-of-contact were hand-polished with gamma aluminum oxide to remove any possible protuberances from the plating process.

Tests were resumed with the low-viscosity oil. Viscosity was varied by temperature control from 5 to 10.5 centipoises, N (speed) was varied from 1,500 r.p.m. to 3,270 r.p.m., and P (pressure) expressed in terms of %Ti (input torque) was varied from 50 to 100. A total of ten cases were tested during three separate runs. ZN/%Ti varied from 112 to 315. These are shown on Figure 17, B1 through B10; the data are summarized in Table III. The high losses associated with turbulence were not observed.

The test development which influenced further testing was that ZN/P could be reduced considerably below the design point with a resultant nonlinear increase in efficiency. "Z" was previously established at 0.6 centipoise as the practical limit of viscosity reduction as a method of improving efficiency. "N" is fixed by design specification at 30,000 r.p.m., and "P" is the remaining variable. Note that losses are inversely proportional to "P", meaning that "P" should be increased. An explanation may be in order. For a given load, a reduction in load-carrying area causes less oil to be sheared, decreasing losses, and results in an increase in "P" (p.s.i.). The load includes input torque load plus flexspline deflection load plus tooth reaction load plus scavenge oil pumping load. The area is the load-carrying quadrants of the wave generator. An increase in P to its feasible limit may be achieved by a reduction in load-carrying area. Any decrease in loads would increase efficiency and permit a further reduction in area to a new feasibility limit. A reduction in area and load involved redesign and rework. The test program was, therefore, directed toward simulating this increase in "P" from reduction in area by keeping input torque at 100 percent, by decreasing Z (viscosity) by temperature increase, and by decreasing N (r.p.m.). R.P.M. was reduced and the temperature was raised until simulation of area reduction reached 38 percent (pressure increase of 61 percent). Further simulated pressure area reduction was twice attempted,

but proved to be unsuccessful in that the oil film became too thin, the surfaces contacted, and the unit stopped. Testing was resumed after both stops with no deterioration apparent. This method of testing gives results limited to parts of similar geometry exposed to similar loads. For instance, contour modification improving film strength in the area of greatest load would allow further length reduction. No light is shed on loss reduction through area removal from more lightly loaded areas. A decrease in bearing diameter, if allowed by flexspline strength and other considerations, would be another method of area reduction of great advantage. The effect of these changes cannot be established by this method of testing. In addition, load reduction can be achieved, as discussed in the next section. Briefly, length reduction reduces secondary portions of the total load by reducing flexspline deflection load and scavenge oil pumping load. Additional secondary load reduction is possible. The effect of these load reductions do not appear as a measurable test result. This method of area reduction, therefore, is applicable only to reduction in length of the bearing without change in load, dictated by film strength in the region of greatest load.

4. Test Results

Results are presented in the form of losses versus ZN/%Ti, Figure 17. These were established by this test program for this test transmission. Table III presents the data involved.

ZN/P is the vonentional parameter used to evaluate hydrodynamic journal bearings. The conventional method of determining "P" is not valid for the harmonic drive, because conventional journal bearings are rigid and the harmonic drive pressure distribution is entirely different. In order to avoid confusion and possible misinterpretation, the parameter used here is ZN/%Ti. Ti is input torque, to which the pressure is directly proportional. This distinction in no way changes the validity of this parameter while it intentionally prevents direct comparison with rigid journal bearing ZN/P curves.

A total of 23 runs were made. Some were for the usual test rig reasons (i.e., to check oil system and oil breather and to calibrate tachometer, etc.), and no data were taken. Other data were discarded because of faulty or unreliable instrumentation, damage occurring at an unknown point in time, or subsequent modification which made the results of little interest. Tabel IV gives a summation of the stress cycles accumulated in the 9-1/2 hours of test time.

Points A-1 through A-4 were obtained with the test transmission, as designed, with the high-viscosity lubricant, Ore Lube K-40. Points B-1 through B-10 were obtained with the test transmission modified and with the low-viscosity lubricant, MIL-O-6081-1010. The modifications included a wave generator length reduction from 6 inches to 4-3/4 inches. 3/8 inch was removed from the input end; 7/8 inch was removed from the output end. In addition, the load-carrying surfaces of the wave generator were electroless nickel plated .0004 inch, heat-treated to Rockwell C-60 (converted).

Points A-1' through A-4' were obtained by reducing the losses by the ratio of 4-3/4 inches/6 inches, a constant factor of 0.792. Good agreement with the B-1 through B-10 curve is noted. This ratio is the ratio of the two-wave generator lengths involved: 6 inches long for A-1 through A-4, 4-3/4 inches long for B-1 through B-10. This implies that losses are directly proportional to length, at least in the straight-line portion of the curve.

The scale design point is noted for the transmission as designed. The scale design points noted for the transmission as redesigned are discussed in the following section.

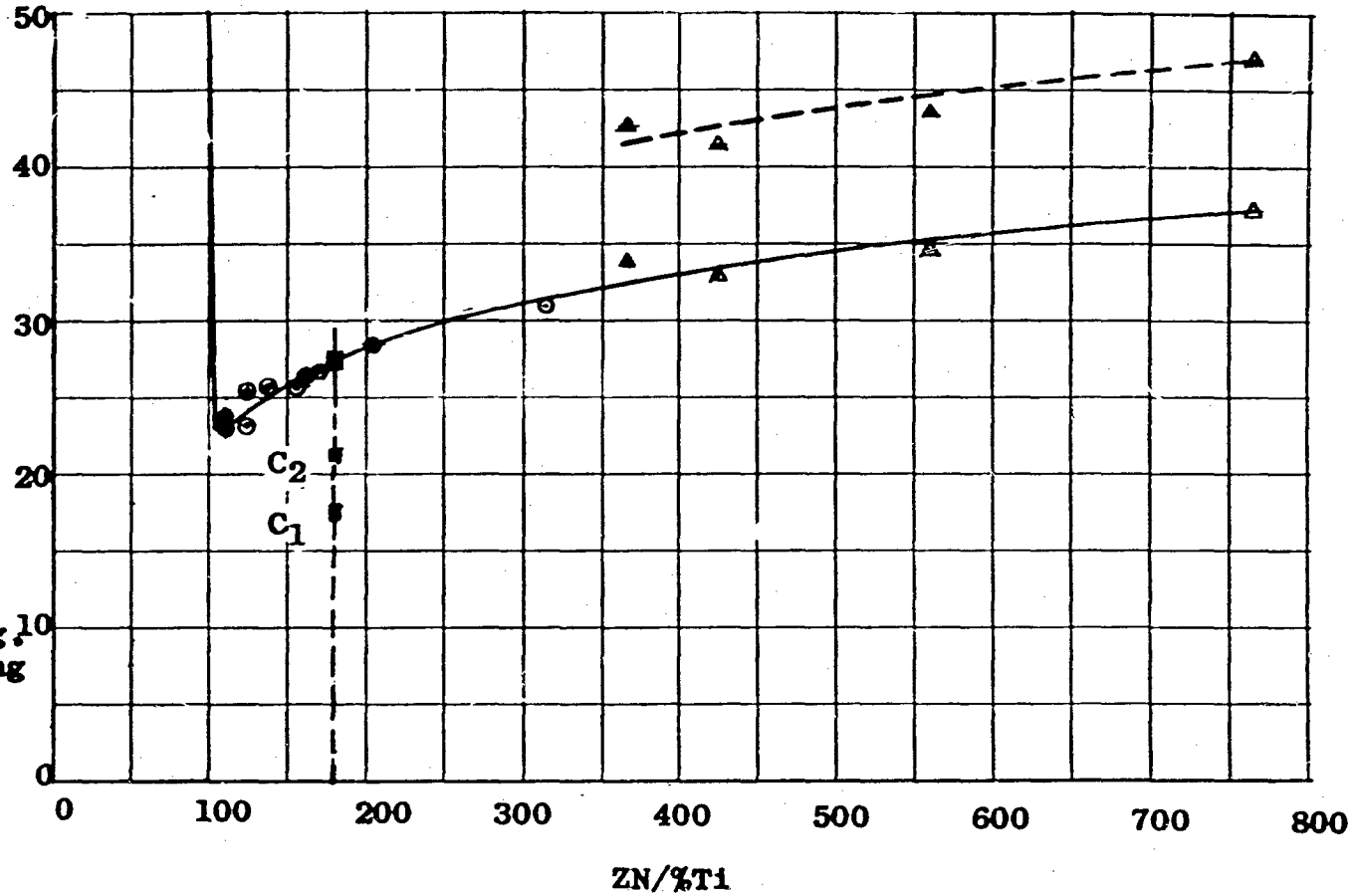

Z = Absolute Viscosity in Centipoises
N = RPM
%Ti = % of Design Input Torque (100=100%)
△---△ = Tests A-1 Through A-4, Ore Lube K-40 Oil
△——△ = Tests A-1' Through A-4', Compensated For Shortened Wave Generator
○——○ = Tests B-1 Through B-10, MIL-O-6081-1010 Oil
——⊡—— = Scale Design Point, Transmission As Designed
C_1, C_2, --⊡-- = Scale Design Point, Improved Transmission (Predicted)

Figure 17. Losses Versus ZN/%Ti

TABLE III

SUMMATION OF TEST RESULTS

Test No.	Losses %	Z Centipoises	N RPM	P %Ti	ZN %Ti	Oil Film Thickness-Inches
A-1	47.0	110	382	55	764	.005+
A-2	43.6	100	392	70	560	.005+
A-3	42.7	96	382	100	367	.005+
A-4	41.5	95	439	98	426	.005+
B-1	31.0	10.5	1500	50	315	-----
B-2	28.5	7.5	2000	74	203	-----
B-3	26.8	5.5	3090	100	170	.004+
B-4	26.5	5.0	3270	100	163.3	-----
B-5	26.0	6.3	2550	100	157.5	.004+
B-6	26.0	5.8	2380	100	138	-----
B-7	25.5	5.7	2220	100	126.5	-----
B-8	23.8	5.6	2000	100	112	-----
B-9	23.3	6.2	2000	100	124	-----
B-10	22.9	5.7	1980	100	112.8	.001

TABLE IV

SUMMATION OF STRESS CYCLES VERSUS LOAD

No Load	276,000
25 Percent Input Torque . . .	100,000
50 Percent Input Torque . . .	253,000
75 Percent Input Torque	17,000
100 Percent Input Torque. . . .	215,000
TOTAL	861,000

5. Critique of Test Unit Design and Test Procedure

Wave Generator - The load-carrying capacity of the hydrodynamic bearing was found to be larger than predicted. The area was found to be reducible by 38 percent. The present wave generator was shortened 7/8 inch at the output end during testing. This resulted in poor support for the flexspline teeth at that end. The wave generator has requirements for shorter length, better axial location, greater surface hardness, greater core toughness, dynamic stiffness with lighter weight, smoother contour at the entrance and exit edges of the load-carrying quadrants, and an incremental increase in surface radii to match a larger flexspline inside diameter (reduced bed thickness); also, it could use a simpler oil distribution system.

Circular Spline - Circular spline length requires consideration of tooth strength. The circular spline teeth are inherently stronger (internal tooth form) than the flexspline teeth (external tooth form).

Flexspline - The flexspline teeth were minutely examined at 45-power magnification. The .003 glass bead tooth cleanup during manufacture appeared as large craters on the tooth surfaces. There was no visible difference between the loaded and unloaded tooth flanks. Isolated marks were visible which may have been wear indications. These were of less depth than the glass bead craters. Apparently, more teeth share the load than was previously believed. This could be due to load transfer to many teeth by oil pumped along the teeth. This also could be due to the operating characteristics of the hydrodynamic bearing, which controls flexspline tooth location (and therefore number of teeth engaged) by lubricant film thickness. The circumferential film thickness distribution is not known and is open to question. There appears to be a self-compensating deflection of the flexspline not included in theory, which may have contributed to the increased capacity of this bearing. This self-compensation would also force tooth load sharing. Without firm knowledge of film thickness distribution, calculations of tooth shear stress cannot be made because the number of teeth sharing the load cannot be established. Tooth strength is not known to be a limiting factor in establishing length or diameter of the flexspline.

Shortening the flexspline causes an increase in tooth bed stress. This can be minimized by reducing the tooth bed thickness. This shortening and thinning have desirable side effects in reducing the flexspline deflection load, increasing efficiency, and reducing starting torque. Reduction in flexspline deflection load could permit further bearing area reduction.

There are three other loads carried by the bearing: scavenge or pumping load, input torque load, and tooth reaction load.

The scavenge oil pumping load will be reduced by a shortened tooth length. The load may be reduced further by better bypass scavenging. This must be done with caution, because the oil pumping may have provided a load transfer mechanism by which many flexspline teeth shared the tooth load.

The input torque load is fixed by wave generator contour and design specifications. The effectiveness of the present contour could be determined with knowledge of the circumferential oil film thickness distribution (discussion below). The self-compensating behavior of the flexspline indicates that an envelope of serviceable contours exists which is wider than theory would indicate. This area of load reduction is dependent on evolving a method of determining circumferential oil film thickness distribution and the effect of contour change on that distribution.

Tooth reaction load includes the tooth separating force, a function of tooth profile, and tooth mesh losses. Some tooth profile other than the present 14-1/2 degree pressure angle involute tooth, might reduce tooth separating force. Tooth mesh losses are theoretically quite small with the harmonic drive, as the teeth reacting output torque are theoretically stationary. Any tooth mesh loss which did occur would be reduced by reduction in length.

Instrumentation - The harmonic drive with a hydrodynamic bearing requires control of oil film thickness. Too thin a film results in film breakdown and bearing contact. Too thick a film results in tooth jamming as the flexspline teeth are forced into too deep an engagement with the circular spline teeth. Major axis film thickness measurement

was necessary and useful, this being the location of greatest load and least film thickness. This was accomplished by insulated probes, mounted radially in the housing, and calibrated for change in capacitance as radial displacement of the flexspline caused a change in the distance between the flexspline and the probes. The change in radial displacement of the flexspline was caused by rotation of the wave generator plus the oil film thickness. Unfortunately, the change in capacitance was nonlinear; and at a distance of over .005 inch, the resolution was insufficient for useful purposes. 0.005 inch is approximately the range of oil film thickness. Therefore, the change in radial displacement of the flexspline from wave generator rotation (approximately .060 inch) effectively eliminated useful data on circumferential oil film thickness distribution. The probes were calibrated to read major axis oil film thickness, essential for safe test operation.

Instrumentation with improved linearity is required in order to measure complete circumferential film thickness distribution and to explore the potential benefits to be gained with this knowledge. These benefits include the various approaches to area reduction and load reduction discussed previously.

Natural Frequency - The natural frequency of the flexspline may be important, although the flexspline is extensively damped by oil under pressure internally and externally. A forcing function will be present at input speed and at twice input speed (caused by the two lobes on the wave generator). Flexspline design should insure that a natural frequency does not occur in close proximity to the forcing functions.

6. Conclusions

This section discusses the results with respect to the goals established for the test program. The goals are used as titles for the respective area.

Goal No. 1 - Establish ZN/P as a suitable parameter for efficiency testing.

The curve shown on Figure 17 indicates that ZN/P is a valid parameter, at least within the limits tested. The input speed varied from 1/100 design speed to 1/10 design speed with consistent results in terms of this parameter. This appears to support the expectation that consistent behavior will occur at design speed.

Goal No. 2 - Determine the practical limit of viscosity reduction as a method of improving efficiency.

Efficiency improvement was not found to be limited by the practical limit of viscosity reduction established for this test program. The lowest practical viscosity material appears to be JP-4 turbine engine fuel, where the viscosity is Z = 0.6 centipoise at 120 degrees F. This limit was used for ZN/P testing. The bearing capacity indicated that a lower viscosity lubricant could be used, if available. Efficiency improvement can be achieved through modification of the other variable in the ZN/P parameter. This takes the form of an increase in "P" (pressure), because "N" (r.p.m.) is fixed by design specifications.

Goal No. 3 - Investigate turbulence as a limiting factor.

Two schools of thought existed on this subject. The velocity viscosity relationship shows that turbulence could be expected. One resulting prediction was that turbulence would occur. The contending opinion was that turbulence-producing conditions (decreasing pressure) would cause a local collapse of the flexspline which would suppress the incipient turbulence. In other words, the flexible nature of the flexspline would provide a separation suppressing mechanism. This difference of opinion established this goal.

The transition number above which turbulence may be expected is calculated for three locations (the major axis, the minor axis, and the unloaded quadrant) with the two lubricants tested.

The general equation for the transition number is:

$$N_T = 1.57 \times 10^3 \frac{v}{D^{1/2} C^{2/3}}$$ Reference 5, page 231

where N_T = Transition r.p.m.

v = Kinematic viscosity inches ^{2}/second

= Viscosity in centistokes x 1.55×10^{-3}

D = Diameter, inches

C = Diametral clearance, inches

The transition number for the high viscosity lubricant, Ore Lube K-40, is calculated at three locations.

Major Axis, .005 + inches film thickness

$$N_T = 1.57 \times 10^3 \quad \frac{120 \times 1.55 \times 10^{-3}}{(5.1214)^{1/2}(.010)^{3/2}} = 128{,}000 \text{ r.p.m.}$$

Minor Axis, assume .010-inch film thickness entrance condition

$$N_T = 1.57 \times 10^3 \quad \frac{120 \times 1.55 \times 10^{-3}}{(4.992)^{1/2}(.02)^{3/2}} = 46{,}800 \text{ r.p.m.}$$

Unloaded Quadrant, .0635-inch film thickness

$$N_T = 1.57 \times 10^3 \quad \frac{120 \times 1.55 \times 10^{-3}}{(4.930)^{1/2}(.1270)^{3/2}} = 2{,}900 \text{ r.p.m.}$$

The transition number is lowest with the low viscosity lubricant, MIL-O-6081-1010, where $v = 7 \times 1.55 \times 10^{-3}$ at 120°F.

Major Axis, .005 + film thickness

$$N_T = 1.57 \times 10^3 \quad \frac{7 \times 1.55 \times 10^{-3}}{(5.1214)^{1/2}(.010)^{3/2}} = 7500 \text{ r.p.m.}$$

Minor axis, assume .010-inch film thickness entrance condition

$$N_T = 1.57 \times 10^3 \frac{7 \times 1.55 \times 10^{-3}}{(4.992)^{1/2}(.02)^{3/2}} = 2,720 \text{ r.p.m.}$$

Unloaded quadrant, .0635-inch film thickness

$$N_T = 1.57 \times 10^3 \frac{7 \times 1.55 \times 10^{-3}}{(4.930)^{1/2}(.1270)^{3/2}} = 169 \text{ r.p.m.}$$

The data shown on Figure 17 establish that the high loss discontinuity associated with turbulence was not observed.

The maximum speed of 380 r.p.m. used with the high-viscosity lubricant is well below the transition speeds calculated above.

The 3,000-r.p.m. speed reached with the low-viscosity lubricant exceeded the calculated transition speeds over a substantial portion of the wave generator surface. The resulting turbulence, if it did occur, was not observed to cause a measurable increase in power loss.

Higher speed testing will be required to obtain valid data establishing turbulence criteria for this unconventional hydrodynamic bearing.

Goal No. 4 - Observe the operating characteristics of this bearing as a novel hydrodynamic bearing approach.

Background - In the harmonic drive, the two lobes of the elliptoidal wave generator (shaft) cause a deflection of the flexspline (bearing) into a similar cross section with a resultant spring load on the major axis and a small gap at the minor axis. Rotation of the wave generator traps lubricant into a converging wedge between the wave generator and the flexspline. This is recognized as a novel bearing type. Therefore, operating characteristics are of interest.

Observed Operating Characteristics

1. Starting torque caused by the spring load on the major axis was reduced. Further reduction may be required for some bearing applications.

2. The converging wedge noted above is apparently modified during operation, tending toward a more uniform film thickness. This is required by the appearance of an oil film at the major axis, assuming no change in circumference of flexspline.

3. End flow effect on the converging wedge is apparently slight. Removal of dams intended to prevent end flow did not affect major diameter oil film thickness.

4. Higher speed testing will be required to determine the behavior of this bearing with respect to turbulence.

Goal Number 5 - Observe the operating characteristics of the harmonic drive test transmission.

The harmonic drive test transmission is fully capable of transmitting the torque required, is quiet in operation, imposes no objectionable vibration characteristics, and appears to have the potential for extreme reliability. The efficiency of the hydrodynamic bearing remains as a key factor limiting feasibility for main speed reduction units in helicopters.

Starting torque was reduced to a high but acceptable level. Further reduction is predicted. The hydrodynamic bearing requires normal attention to cleanliness. Power must be increased or decreased within an envelope of speed/torque ratios to keep the lubricant film thickness within acceptable limits. Adding a hydrostatic feature to the basic hydrodynamic bearing could prove useful in widening this envelope by removing the limit imposed by film breakdown from too high a torque for a given speed. It would also reduce starting torque further.

Goal Number 6 - Predict expected efficiency of harmonic drives with hydrodynamic bearings through scale testing for the power spectrum of the parametric analysis, 250 to 4,000 horsepower. (Considerations noted elsewhere limit this prediction to the present state of the art.)

The test data show the loss at the scale design point to be 27.5 percent. The data indicate that the load-carrying area can be reduced by approximately 38 percent. Two methods of calculation based on test data are used to estimate the reduced losses. One is selected as more firmly substantiated. Neither includes considerations other than area reduction by simulated length reduction. This prediction is therefore limited to those values for which test substantiation and conservative analysis can be offered. It is felt that this defines the present state of the art. The harmonic drive parametric analysis is then re-entered. Predictions are made for the power spectrum of 250 horsepower to 4,000 horsepower, Figure 18. The evaluation of these predictions is presented graphically under Section V, Program Discussion, pages 8 to 15.

The first method of predicting losses for an improved transmission is based on the test data shown on Figure 17. The losses at Points A-1 through A-4 were obtained with a wave generator length of 6 inches. The losses at Points B-1 through B-10 were obtained with a wave generator length of 4-3/4 inches. The reduction in length caused a displacement of the curve in the direction of reduced losses. The relationship found to produce agreement was to multiply losses at Points A-1 through A-4 by the inverse ratio of the lengths, 4-3/4 inches/6 inches, or a constant factor of 0.792. The loss at the design point is not in the essentially straight-line portion of the curve where this relationship is found. The length ratio method is not proven valid at the design point. With this reservation in mind, the loss ratio to be expected with the reduced length is 3 inches/4-3/4 inches, or a constant factor of 0.632. The loss at the design point is given by 27.5 percent x 0.632 - 17.4 percent. This was shown at C_1 on Figure 17. This point is shown at C_1 on Figure 18.

The second method is to use the Kingsbury thrust bearing analogy, as used in the original performance calculations. The general equation is found in Reference 4, page 329.

$$\text{Horsepower Loss} = K_6 \frac{\left(\frac{\mu U}{PB}\right)^{1/2}}{550 \times 12} \qquad \text{PLBU} = \frac{K_6 L \sqrt{\mu P B U^3}}{6600}$$

The variables to be investigated are L = length in inches and P = pressure (p.s.i.). All others remain constant (Q).

$$\text{Loss} = Q\ L\ \sqrt{P}$$

Let Loss_1 = Loss for test unit

Loss_2 = Loss for improved unit

L_1 = 4 3/4-inch wave generator

L_2 = 3-inch wave generator

P_1 = Pressure on 4 3/4-inch wave generator

P_2 = Pressure on 3-inch wave generator

$$\text{Then, } \text{Loss}_2 = \text{Loss}_1 \times \frac{L_2}{L_1} \sqrt{\frac{P_2}{P_1}}$$

The term P_2/P_1 can be written in terms of L_1 and L_2, because pressure is inversely proportional to length. Another factor must be considered. Reducing the length of the flexspline reduced the total load by 6 percent. The pressure ratio in terms of length is given by:

$$\text{Loss}_2 = \text{Loss}_1 \frac{L_2}{L_1} \sqrt{\frac{.94\ L_1}{L_2}} = \text{Loss}_1\ (.772)$$

The loss at the design point is then 27.5 percent x .772 = 21.2 percent. This was shown at C_2 in Figure 17. This point is shown at C_2 in Figure 18.

Loss at the design point should be less than this predicted range. The total pressure used in these analyses did not consider load reduction from reduced scavenge oil pumping load. The tooth mesh losses are also reduced with the shortened proportions.

It is of interest to note that these analyses predict losses between 17.4 percent and 21.2 percent for the shortened wave generator, while the test simulating this reduction in length showed 23 percent loss. The higher simulated loss is believed due to two reasons: the inability to simulate the reduction in load from a shortened flexspline, and the reworked condition of the wave generator. The wave generator was originally 6 inches long, but was reworked until the effective length was 4-3/4 inches. The unused length, although below contour, may have contributed added drag.

The harmonic drive parametric analysis provided calculated efficiency versus output horsepower for two film thicknesses, Curve H (thick film) and Curve I (thin film). This is shown in Figure 14; data are given in Table I. Input horsepower is the more conventional and perhaps more useful comparison. The Table I data were therefore used to plot Curves K and L in Figure 18. These curves show calculated efficiency versus input horsepower for the thick and thin film cases, respectively. Input horsepower was obtained by adding output horsepower and losses.

The test transmission loss: C - thick film, C' - thin film and calculated losses associated with an improved transmission, C_1 and C_2, are plotted in Figure 18. The chief point of interest is the agreement between the calculated Point C_1 and Curve L. C_1 was calculated using the length ratio method for which experimental justification is tentatively established, whereas C_2 is based on analogy. It is felt that the agreement of C_1 with Curve L establishes an experimentally based confirmation of the point of origin of Curve L. The validity of the trend of Curve L rests on the torque-speed values determined in the parametric analysis and the calculated harmonic drive performance characteristics using those values. The power loss equation was derived in general form in the Parametric Analysis, VI C.

Horsepower Loss = (Constant)(Output Torque)$^{5/6}$ (Input Speed).

This general equation is believed to be correct. The Point C_1 then verifies the derived constant, giving the specific power loss equation for helicopter main speed reduction units:

Horsepower Loss = 2.3×10^{-7} $(T_O)^{5/6}$ (N_I).

The conclusion reached is that sufficient justification exists for the use of Curve L to predict expected efficiency.

Table V shows the losses so established.

TABLE V

EFFICIENCY PREDICTION DATA

Input Horsepower	Efficiency	Losses
250	82.6	17.4
1000	86.3	13.7
2000	88.2	11.8
3000	89.3	10.7
4000	89.7	10.3

NOTE:

This prediction is limited to those values for which test substantiation and conservative analysis can be offered. It is felt that this defines the present state of the art. Significant improvement is anticipated.

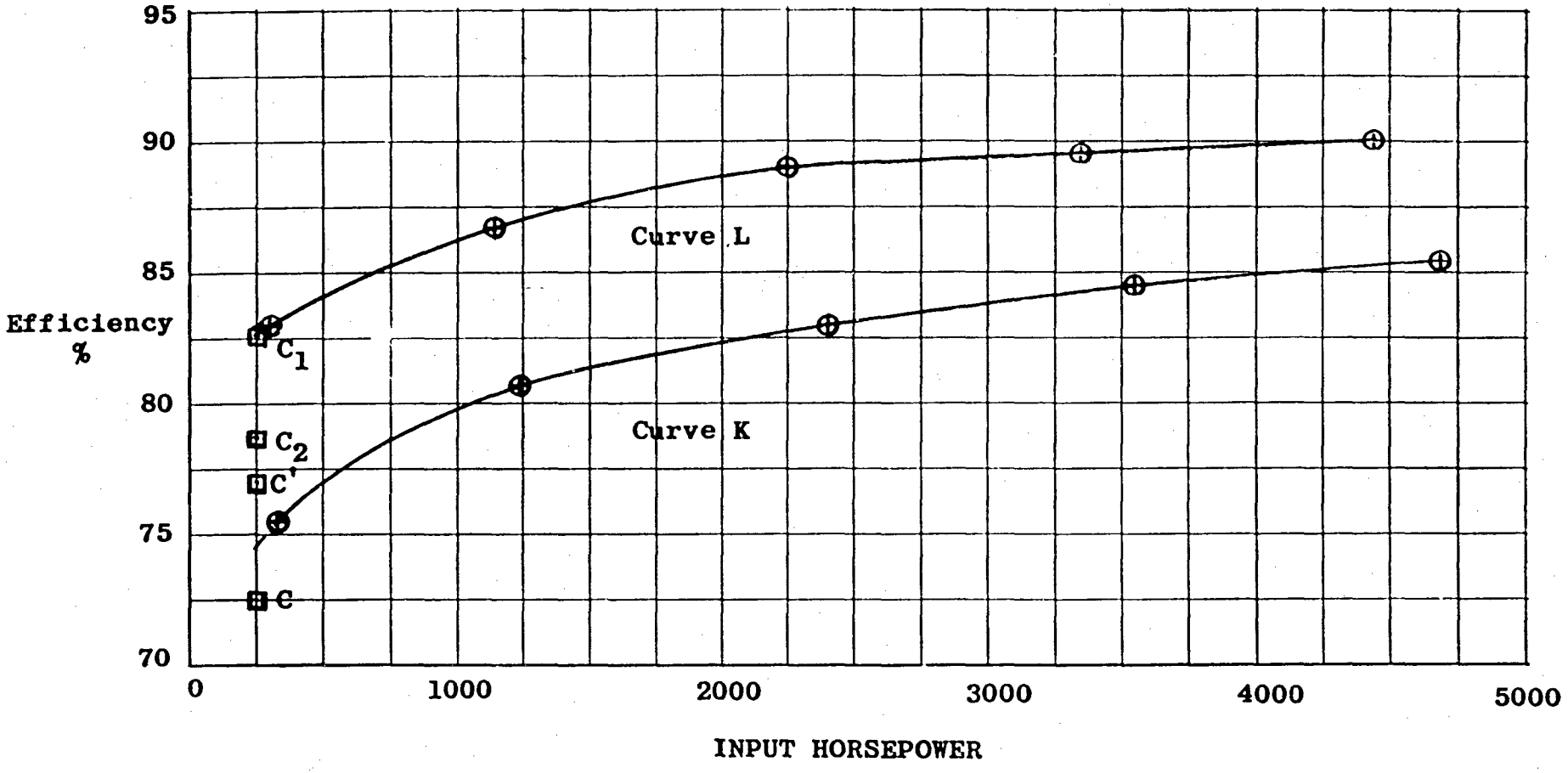

Curve K - Calculated Performance, Thick Film (.0015 inches at 250 HP), Table I Data
Curve L - Calculated Performance, Thin Film (.0010 inches at 250 HP), Table I Data
C, Test Transmission Scale Performance, Thick Film (.004+ inches)
C' Test Transmission Scale Performance, Thin Film (.001 inches)
C_1 Calculated Thin Film Performance of Improved Transmission Using Length Ratio Method
C_2 Calculated Thin Film Performance of Improved Transmission Using Kingsbury Thrust Bearing Analogy

FIGURE 18. Efficiency Versus Input Horsepower

BIBLIOGRAPHY

1. Jennings, F. B., Harmonic Drive Hydrodynamic Bearing, United Shoe Machinery Corporation, Boston, Massachusetts, 1963, pp. 1-49.

2. Musser, C. W., "The Harmonic Drive: Breakthrough In Mechanical Drive Design", Machine Design Article, Penton Publishing Company, Cleveland, Ohio, 14 April 1960.

3. Roark, R. J., Formulas For Stress And Strain, Third Edition, McGraw-Hill Book Company, Incorporated, New York City, New York, 1954, pp. 175, 343.

4. Shaw, M. C., and Macks, E. F., Analysis And Lubrication Of Bearings, First Edition, McGraw-Hill Book Company, Incorporated, New York City, New York, 1949, pp. 326, 329, 332-335.

5. Wilcock, D. F., and Booser, E. R., Bearing Design And Application, First Edition, McGraw-Hill Book Company, Incorporated, New York City, New York, 1957, pp. 231, 331.

6. Harmonic Drive Principles And Performance, United Shoe Machinery Corporation, Boston, Massachusetts, 1959, pp. 1-15.

Project 9R-38-01-020-04(P)
Contract DA 44-177-TC-718

September, 1962

APPENDIX

INVESTIGATION OF BOUNDARY LAYER LUBRICATION

KAC Report G-148

Prepared By

Kaman Aircraft Corporation
Bloomfield, Connecticut

For

U.S. Army Transportation Research Command
Fort Eustis, Virginia

TABLE OF CONTENTS

LIST OF ILLUSTRATIONS

LIST OF TABLES

I. SUMMARY

This report describes component sample testing performed in an effort to improve the efficiency of boundary layer lubrication for a harmonic drive transmission with a hydrodynamic bearing.

The theory pusused was that a surface composed of many separate, small reservoirs would present a discontinuous escape path to the lubricant under pressure, thus providing greater film strength and reducing friction.

This theory was confirmed for this application. The theory was also amplified by this program to include an additional requirement that the pocketing effect be achieved by plastic deformation, not erosion, for greater improvement.

II. INTRODUCTION

The purpose of this program was to test a theory which would improve boundary layer lubrication characteristics of the harmonic drive wave generator/flexspline hydrodynamic bearing. This improvement is necessary in order to reduce starting friction. Improvement is also necessary to permit hydrodynamic bearing operation to approach the incipient boundary layer zone where efficiency is greatest.

The theory for achieving this improvement is that to operate in this regime, smoothness of these surfaces is not nearly as important as a nondirectional pocketed surface. There are two reasons, as follows:

1. A pocketed surface offers a discontinuous escape path to the lubricant under pressure, but a ground surface any rougher than RMS-2 has continuous valleys which let the lubricant escape, thus loading up the peaks.

2. The surface is a series of pockets which are lubricant reservoirs. Dynamic behavior of the lubricant in the reservoirs and the effect of this behavior are postulated below.

The small reservoirs are believed to support low-velocity loads by internal circulation of trapped lubricant. As the upper layer in a reservoir is dragged in the direction of motion of the adjacent sliding surface, the lower layer in the reservoir must move in the opposite direction. This circulation is a trapped vortex generated by the motion of fluid adjacent to the surface. Two pocketed surfaces under relative motion and facing each other, with an intervening lubricant film, should then have trapped vortices which are similar in hand but with opposed velocity vectors in the film. These opposed vectors add an aiding velocity component to the fluid in return for the energy required to generate them. This may be an efficiency improving exchange. Some evidence exists to support this thesis. In any event, metal-to-metal contact should be delayed by these trapped vortices.

It is believed that these reservoirs are quite sensitive to entrant and salient angles, at least at the downstream and upstream edges, and that the optimum may depend on many variables, including the properties of the lubricant. It is also believed that an optimum combination may require that a differential exist in the relative size of the reservoirs on each surface. The most desirable selection of surfaces is defined for this program as the lowest starting-friction combination.

This theory is based on evidence from scattered sources and is not described in the literature. Differential materials and differential hardness are quite extensively covered, but are not appropriate to this program at this time. The parts are similar in material and hardness. Depositing soft material on one surface to achieve differential materials seems to be ruled out by a large static line-contact load present in the harmonic drive. This load is imposed by deflecting the flexspline from a circular cross section to an elliptical cross section to accommodate the wave generator. It is felt that a soft material would be scuffed off during assembly or after a few starts. Differential hardness should wait until cam shape is tested but may very well be appropriate at a later date. It should be noted that much of the success with differential materials and differential hardness may be because the successful combinations automatically produce desirable surface reservoir characteristics.

The test program was not an attempt to explore the effects of the ranges of variables involved in developing design criteria. The bearing application is quite specific and the tests reflected this situation.

There were two areas of testing:

1. Tests of methods for achieving a desired range of surface finishes.

2. Tests to find the optimum combination of surface finishes.

III. TEST OF METHODS FOR ACHIEVING DESIRED RANGE OF SURFACE FINISHES

A. PROCEDURE

Test samples were prepared which simulated the wave generator and flexspline bearing surfaces. These samples, all cut from the same piece of bar stock, were the same as expected for the bearing surfaces with respect to material (SAE 4340 steel), hardness (Rockwell C36 to 39), and surface finish (smoother than RMS 8). The samples were disks 1-1/2 inches in diameter and 1/2-inch thick. These samples were glass bead peened using five different bead diameters (.003, .007, .013, .020 and .028 inch), with three different intensities (measured with Almen strips), for a total of thirty samples peened. Twenty additional samples were retained unpeened, some to be used for friction testing of ground surfaces and some to accompany the actual parts during peening as inspection samples.

B. RESULTS AND DISCUSSION

The results of the peening are given in Table I, page 90. The results for Samples 1 and 2 are as recorded, but would be more understandable if inverted. Possibly human error is involved.

C. CONCLUSIONS

1. At this hardness level, glass bead peening did not reduce surface roughness.

2. A pocketed surface was produced as desired.

3. Considerable variation in bead size, intensity, and impingement angle can produce a desired RMS finish.

TABLE I

RESULTS OF GLASS BEAD PEENING

No.	Bead Size	Angle	Intensity	RMS Before	RMS After
1	.023	45	$2A_2$	7	35
2	.028	45	$3.5A_2$	6	15
3	.028	45	$5A_2$	7	59
4	.028	90	$3A_2$	4	18
5	.023	90	$6A_2$	5	38
6	.028	90	$9A_2$	6	56
7	.020	45	$6N_2\ 2A_2$	6	50
8	.020	45	$16N_25A_2$	5	42
9	.020	45	$15N_25A_2$	4	42
10	.020	90	$10N_23A_2$	5	33
11	.020	90	$10N_26A_2$	4	60-40 edges
12	.020	90	$30N_29A_2$	6	42
13	.013	45	$5N_21A_2$	4	20
14	.013	45	$13N_23A_2$	5	36
15	.013	45	$14N_23A_2$	4	50
16	.013	90	$8N_22A_2$	5	20
17	.013	90	$16N_26A_2$	4	51

TABLE I (Continued)

No.	Bead Size	Angle	Intensity	RMS Before	RMS After
18	.013	90	$24N_2 8A_2$	6	51
19	.007	45	$6N_2\ 2A_2$	3	10
20	.007	45	$7N_2\ 2A_2$	6	22
21	.007	45	$9N_2\ 3A_2$	5	22
22	.007	90	$6N_2\ 2A_2$	5	15
23	.007	90	$12N_2 3A_2$	5	30
24	.007	90	$18N_2 5A_2$	5	37
25	.003	45	$3N_2\ 0A_2$	4 wrong side peened	16
26	.003	45	$4N_2\ 2A_2$	5	18
27	.003	45	$8N_2\ 3A_2$	5	29
28	.003	90	$4N_2\ 2A_2$	5	18
29	.003	90	$8N_2\ 3A_2$	5	17
30	.003	90	$12N_2 4A_2$	4	28

IV. TEST TO FIND OPTIMUM COMBINATION OF SURFACE FINISHES

A. PROCEDURE

The test was conducted with the apparatus shown in Figures 1 and 2. This is a starting friction test with a rotating disk on a nonrotating disk. The tests were run with MIL-O-6081-1010 oil, which has low viscosity appropriate for the harmonic drive test program.

Uniform face loading of the disks was provided by the O-ring support for the nonrotating disk and the ball-and-socket loading of the rotating disk. This eliminated any effects of nonparallelism among surfaces.

Variations in disk thickness were accommodated in the following manner. The deflected position of the loading bar which produced the desired load on a weighing scale became the gage height for that load (see Figure 2). After the disks were loaded, the wedges were adjusted, in or out, until the loading bar reached gage height. Loading bar location was checked before and after every test. Gage height was checked for the load supplied after each series. The error introduced by the friction in the ball and socket was quite small and apparently constant. The tests involving a ground surface bearing against another ground surface were always started with the lays parallel.

When two loaded surfaces have moved, several changed conditions exist. For example, friction raises the oil temperature which lowers viscosity so that a repetition of the test will not result in the same numbers. Oil temperature within a bearing tends to remain constant after some initial build-up. This test was conducted by cycling the moving arm back and forth rapidly to bring the oil to a stable temperature, then measuring starting friction.

Starting friction was defined as that value which would cause the moving arm to move from stop to stop two out of three times. It is felt that this technique suppressed the fringe variables sufficiently to reveal significant trends. The values found were repeatable within 10 percent.

Every effort was made to preserve cleanliness. Each part was cleaned with solvent before each test. After this evaporated completely, oil was placed on the disk with a glass tube. The oil supply was always kept covered. After each test, the oil was removed and examined for wear particles.

Each test was completed within one day to avoid large variations in ambient conditions.

Tests were conducted at 50 p.s.i. and 100 p.s.i. The 50-p.s.i. tests were conducted on three separate occasions, followed by the 100-p.s.i. test. The results from the three 50-p.s.i. tests were consistent. The 100-p.s.i. test was conducted to indicate the effect of increasing pressure, decreasing viscosity, or increasing temperature. Each of these moves the surfaces closer together, but increased pressure is easiest to control. The last 50-p.s.i. test and the 100-p.s.i. test are reported here.

The static load on the wave generator is calculated as 50 p.s.i. average and 80 p.s.i. peak, based on a calculated area of contact. The test results are thus germane to this problem.

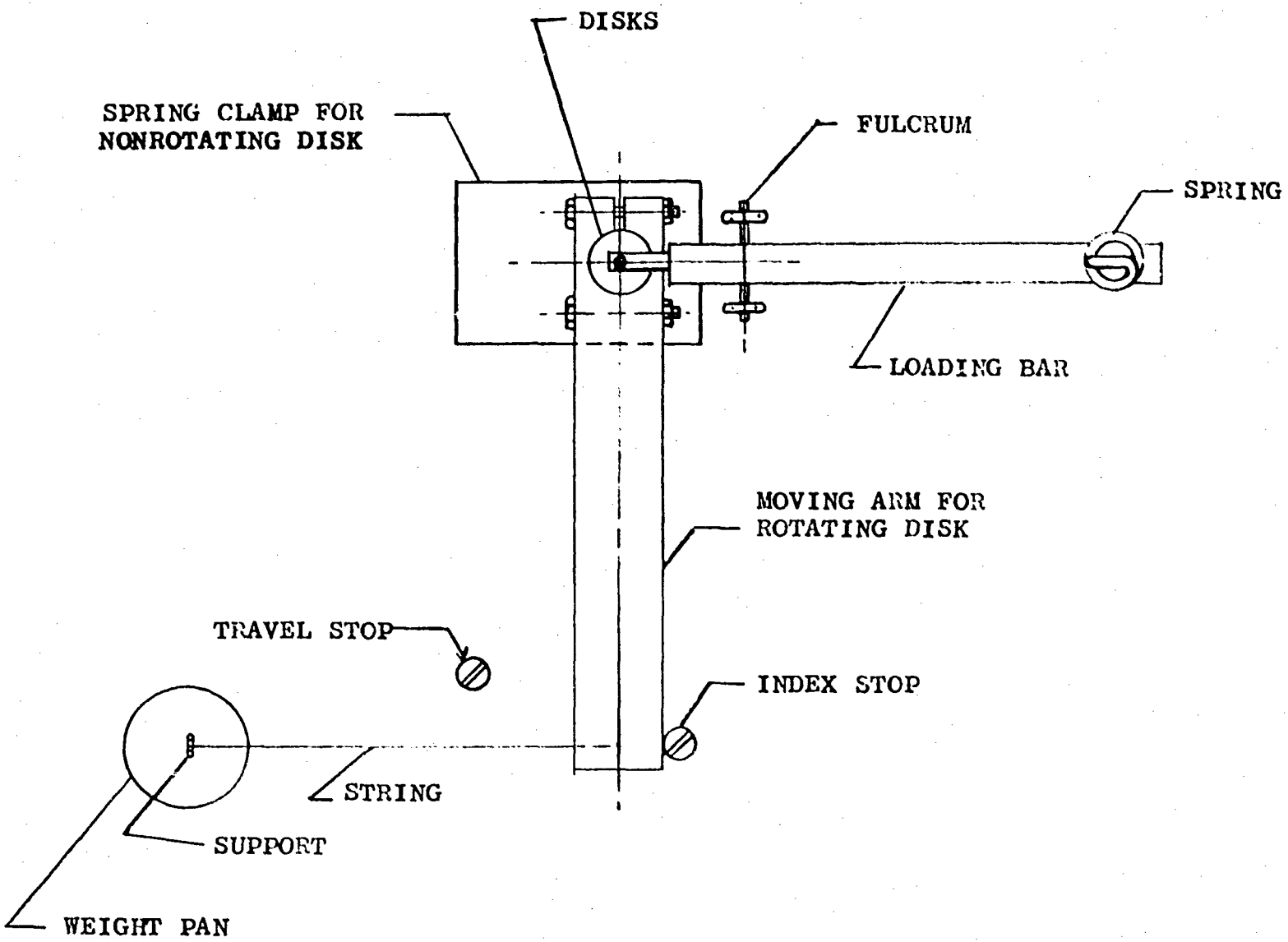

Figure 1. Top View of Test Apparatus

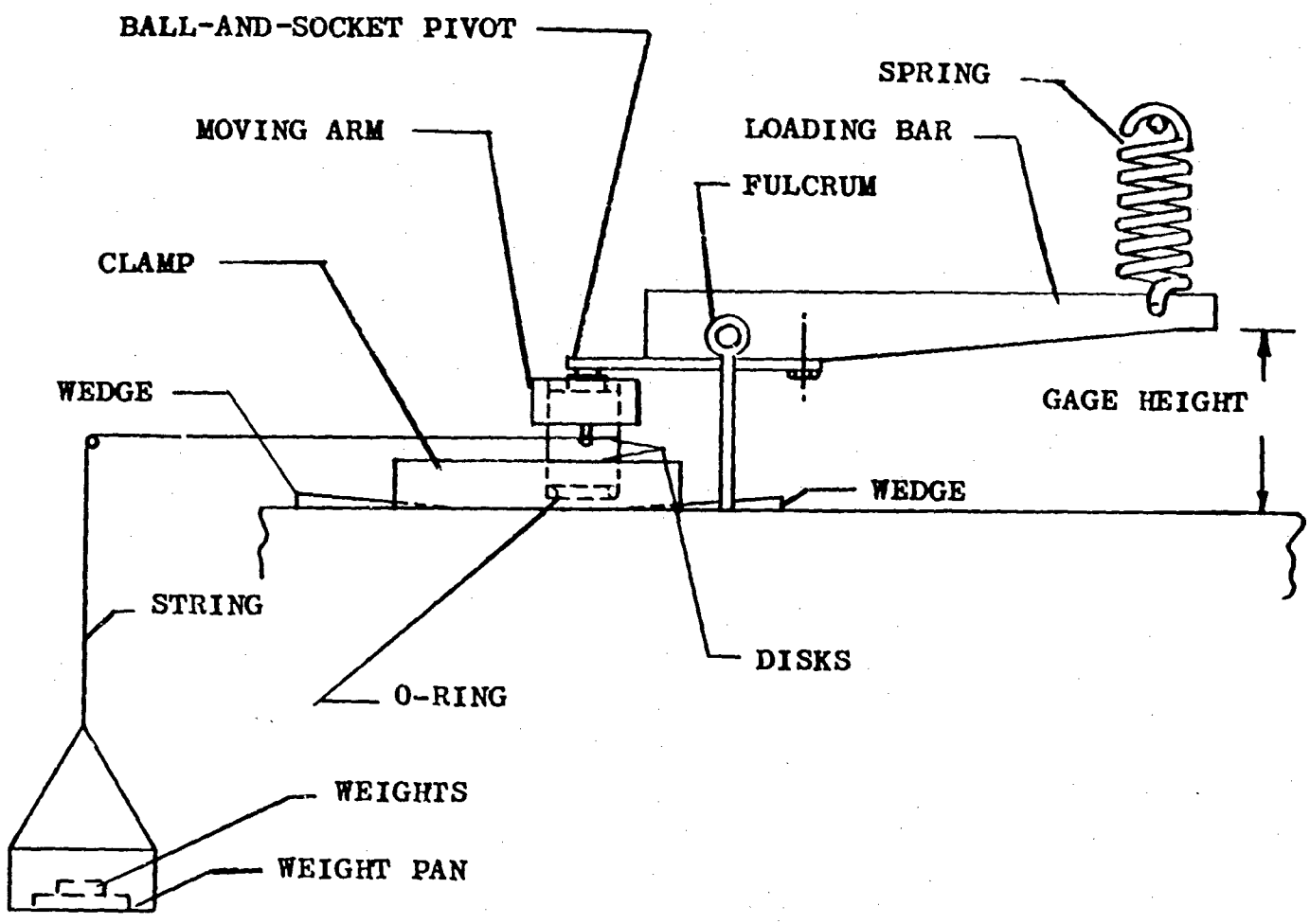

Figure 2. Side View of Test Apparatus

B. RESULTS

The results are shown graphically in Figures 3, 4, 5, 6, 7, and 8. The only effect not shown is wear particles in the oil after testing. These were consistently found with RMS 28; occasionally, with RMS 22 and 30.

C. DISCUSSION

The most obvious feature of the results is the two low-friction zones. These results permit little choice in treatment to be applied. The choice is RMS 10 to 15 on the wave generator to be applied with a .007-inch-diameter bead and RMS 35 to 40 on the flexspline. The bead size chosen for the flexspline was a .020-inch diameter rather than a .028-inch diameter because the results of the glass bead peening tests indicate that a greater spread of intensity is available to achieve this result. This ratio has the following advantages:

1. Least friction.

2. More easily produced than other combinations.

The problem remains of explaining the high friction found at RMS 22 to 28. The data were plotted by ratio of bead size, ratio of RMS, and ratio of intensity, with no correlation.

The possibility of error from unknown factors was investigated. This is single-sample testing, which is always suspect. No deviations such as concavity or convexity could be found. It can be observed that single-sample deviations would be unlikely to produce the trends observed. The errors would have to be in the proper sequence at the proper values in at least four adjacent test specimens to cause this result.

An attempt was made to observe the least angle of contact of this oil on these surfaces. This is a significant measure of surface tension and thus capillary force. The oil was found to be of great spreadability, and the angle of contact approached zero; no significant difference was observed.

It was concluded that RMS is not the quality which describes the property of the surface causing reduced friction, although it can control the processes which produce the desired properties.

Correlation was found for one process variable: effective velocity.

Intensity is a measure of work done which is equivalent to kinetic energy absorbed.

$$\text{Kinetic Energy} = 1/2\ mv^2$$

For kinetic energy, substitute measured intensity (Table I, A_2 values).

For 1/2m, substitute bead diameter cubed (a simplifying proportionality).

A number proportional to effective V, $V_p = \dfrac{\text{Intensity}}{d^3}$.

The plot of averaged starting torque (lowest 3 values at 100 p.s.i. versus V_p is given in Figure 9).

Effective velocity seems to be an indicative parameter for the plastic deformation effect discussed below; however, too low a V_p does not result in sufficient deformation, as noted.

With 50-power magnification, the lowest friction surfaces were observed to be those with plastic deformation and the highest were those with eroded surfaces. The surface of the specimen at RMS 38 was a series of shallow, saucer-shaped depressions. The original ground surface had parallel peaks and valleys. These were no longer raised but were still visible as a flat pattern within the saucers. A much smaller craterlike pocketing was superimposed, apparently from broken beads. None of the original surface structure was visible at RMS 51, although the same bead size had been used. The surface at RMS 28 was a matte of tiny craters. The surfaces at RMS 10 to 18 all showed original surface which had been flattened. Plastic deformation is an added requirement unknown at the origin of this program. This quality seems to be more important than bead size, impingement angle, or intensity.

Another quality of the surfaces was observed which is proportional to friction. The brighter the surface, the lower the friction. The low-friction surfaces sparkled under lighted magnification, but the high-friction surfaces were uniformly dull. The reason for this phenomenon is not known, although it may relate to plastic deformation.

D. CONCLUSIONS

1. Starting friction may be reduced by a surface composed of non-interconnected lubricant reservoirs of appropriate size and shape for that lubricant, which are formed by plastic deformation of the surface.

2. The results of this test program are known to be applicable to starting friction for SAE 4340 steel on steel with a hardness of Rockwell C36 to 39, surface finish as noted, lubricated with MIL-O-6081-1010, and loaded with 50 to 100 p.s.i. Whether variations of these conditions will affect performance is unknown.

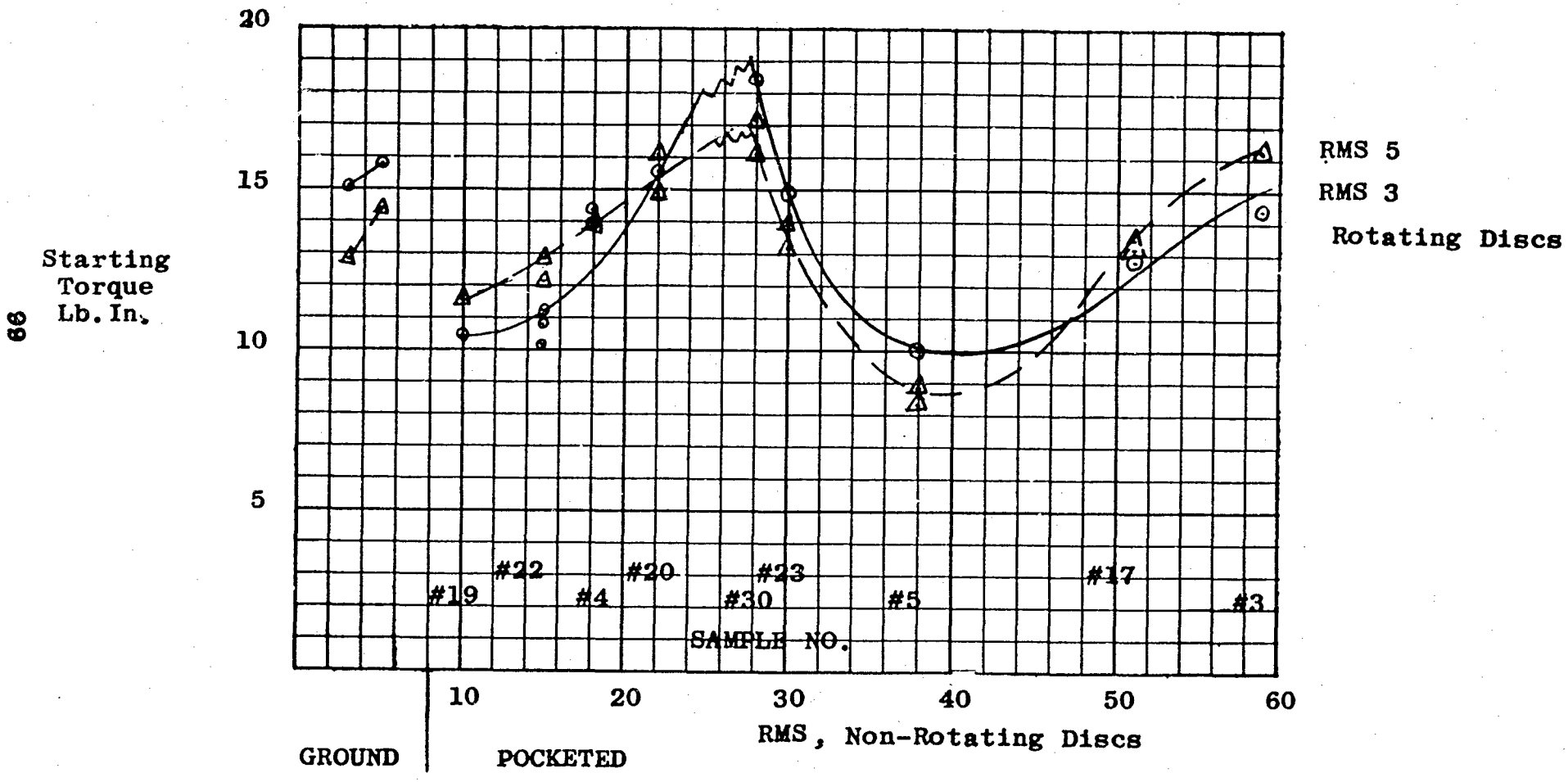

Starting torque found with rotating discs of RMS 3 and 5 on non-rotating discs of various RMS

Figure 3. 50 P.S.I., Starting Torque Versus RMS

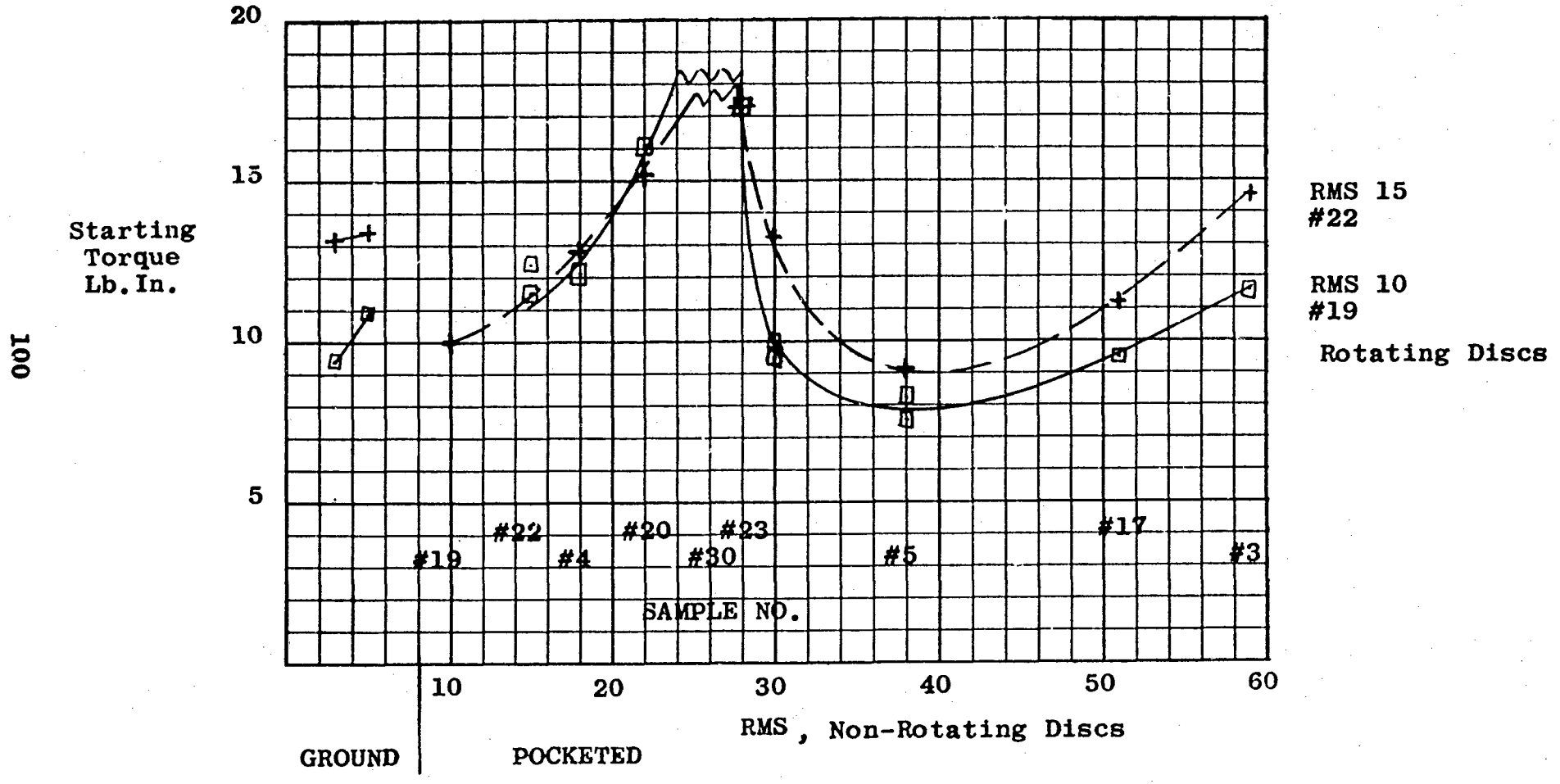

Starting torque found with rotating discs of RMS 10 and 15 on non-rotating discs of various RMS

Figure 4. 50 P.S.I., Starting Torque Versus RMS

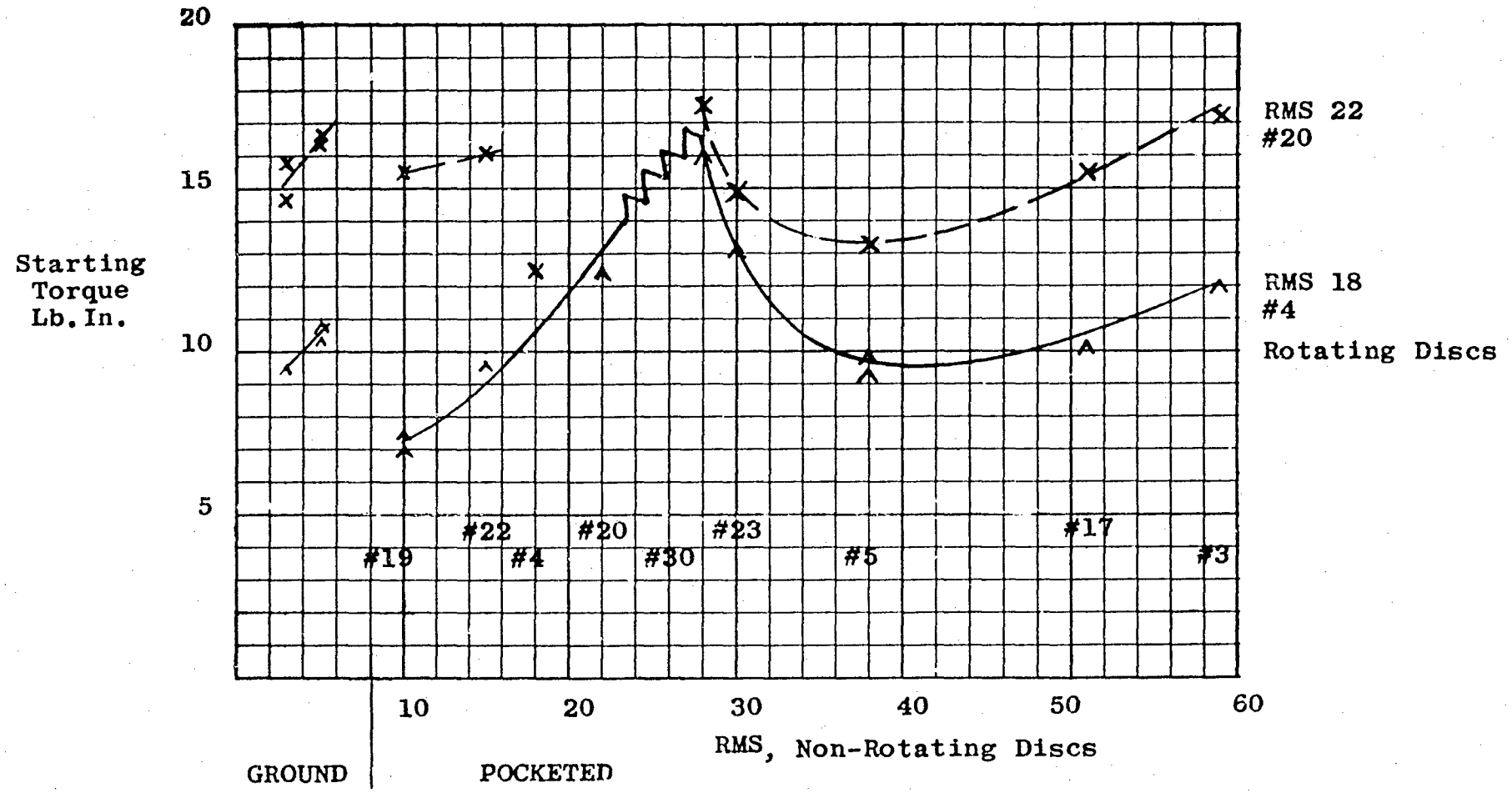

Starting torque found with rotating discs of RMS 18 and 22 on non-rotating discs of various RMS

Figure 5. 50 P.S.I., Starting Torque Versus RMS

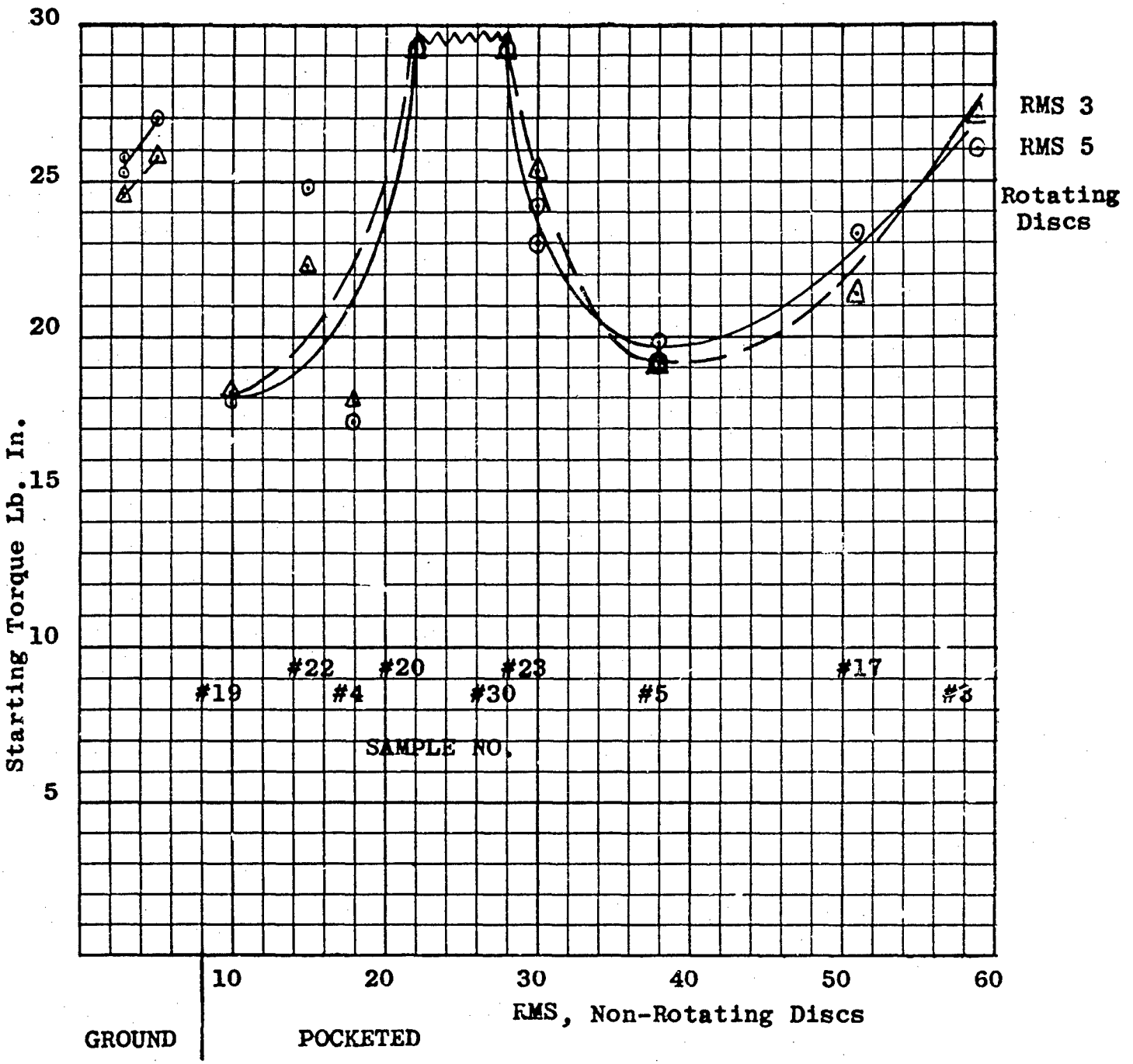

Starting torque found with rotating discs of RMS 3 and 5 on non-rotating discs of various RMS

Figure 6. 100 P.S.I., Starting Torque Versus RMS

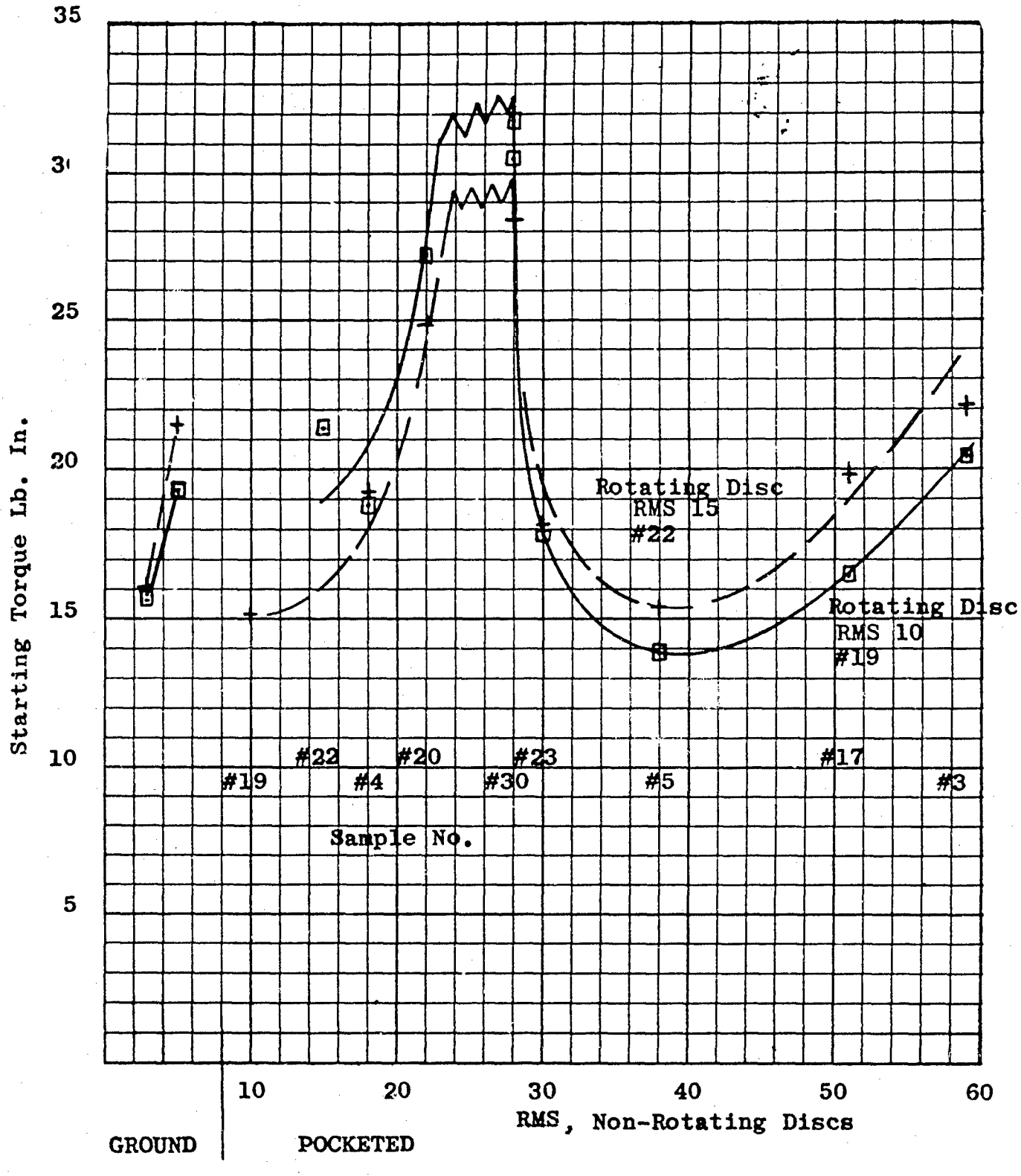

Starting torque found with rotating discs of RMS 10 and 15 on non-rotating discs of various RMS

Figure 7. 100 P.S.I., Starting Torque Versus RMS

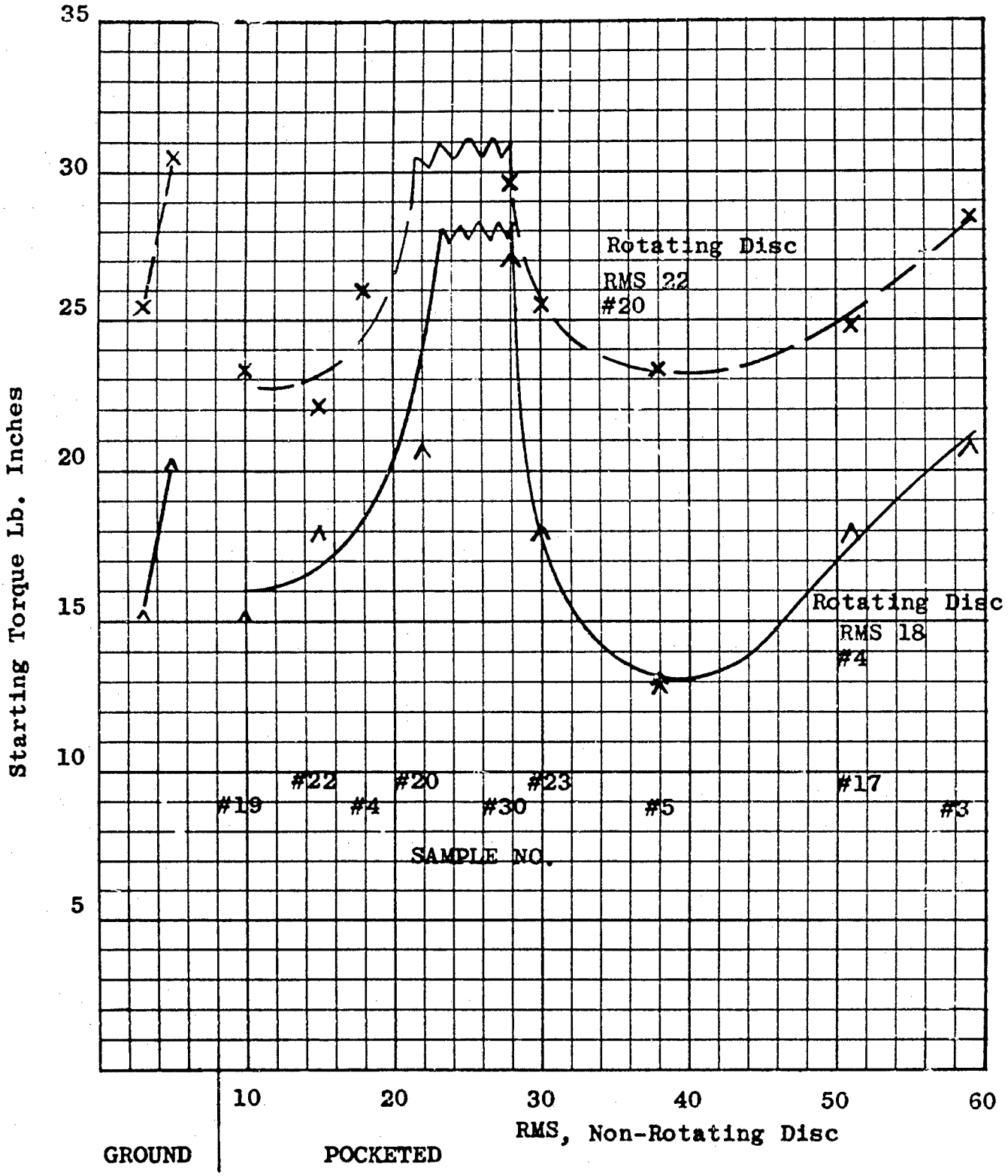

Starting torque found with rotating discs of RMS 18 and 22 on non-rotating discs of various RMS

Figure 8. 100 P.S.I., Starting Torque Versus RMS

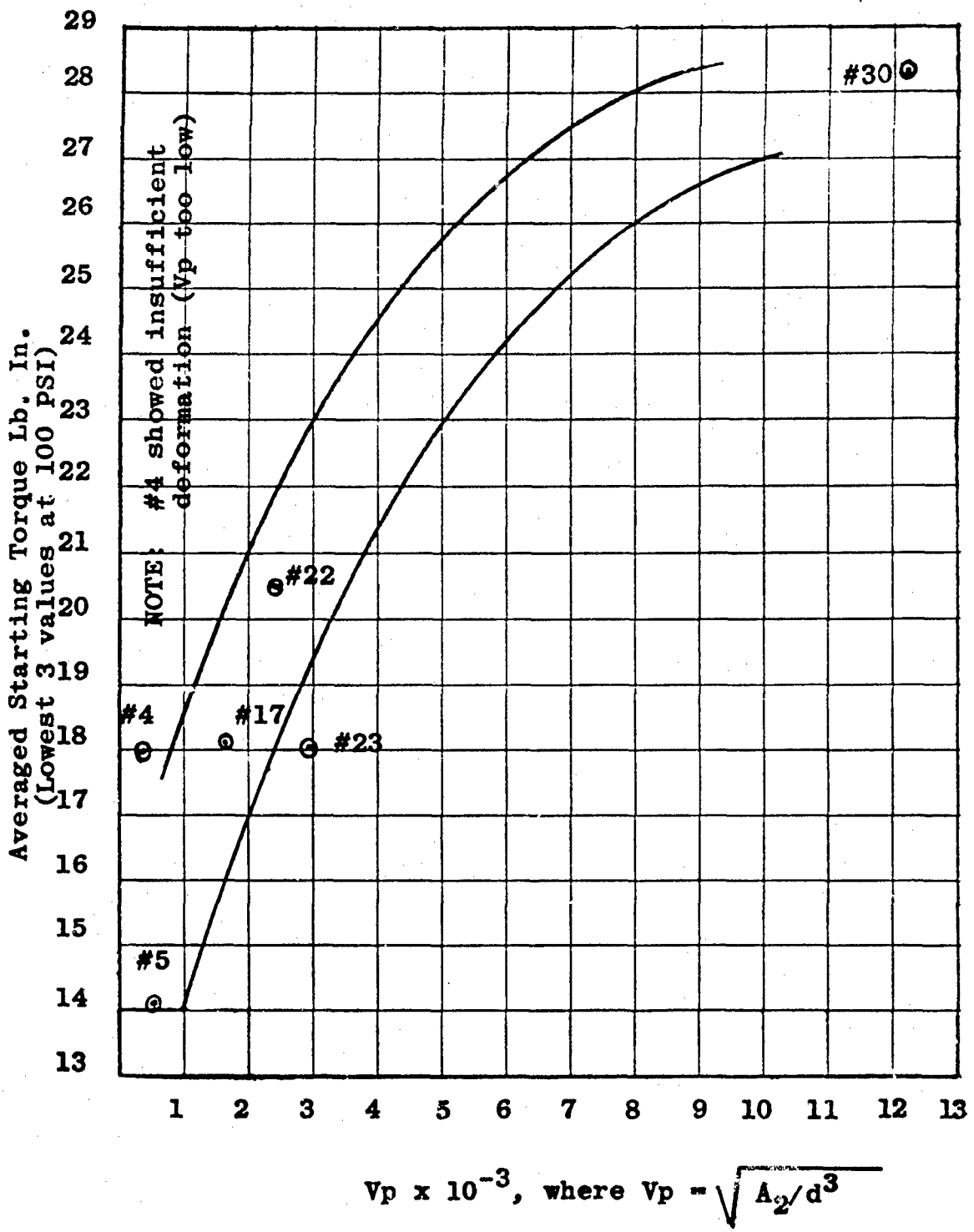

Figure 9. Averaged Starting Torque Versus $V_p \times 10^{-3}$